US 20150148623A1

(19) **United States**

(12) **Patent Application Publication**

Benaron

(10) **Pub. No.: US 2015/0148623 A1**

(43) **Pub. Date: May 28, 2015**

(54) **HYDRATION MONITORING SENSOR AND METHOD FOR CELL PHONES, SMART WATCHES, OCCUPANCY SENSORS, AND WEARABLES**

(71) Applicant: **David Alan Benaron**, Portola Valley, CA (US)

(72) Inventor: **David Alan Benaron**, Portola Valley, CA (US)

(21) Appl. No.: **14/552,690**

(22) Filed: **Nov. 25, 2014**

Related U.S. Application Data

(60) Provisional application No. 61/908,926, filed on Nov. 26, 2013, provisional application No. 61/970,667, filed on Mar. 26, 2014, provisional application No. 61/989,140, filed on May 6, 2014, provisional application No. 62/050,828, filed on Sep. 16, 2014, provisional application No. 62/050,900, filed on Sep. 16, 2014, provisional application No. 62/050,954, filed on Sep. 16, 2014, provisional application No. 62/053,780, filed on Sep. 22, 2014.

Publication Classification

(51) **Int. Cl.**

A61B 5/00	(2006.01)
A61B 5/1455	(2006.01)

(52) **U.S. Cl.**

CPC ***A61B 5/0059*** (2013.01); ***A61B 5/1455*** (2013.01); ***A61B 5/443*** (2013.01)

(57) **ABSTRACT**

An improved sensor (**102**) for hydration monitoring in mobile devices, wearables, security, illumination, photography, and other devices and systems uses an optional phosphor-coated broadband white LED (**103**) to produce broadband light (**114**), which is then transmitted along with any ambient light to target (**125**) such as the ear, face, or wrist of a living subject. Some of the scattered light returning from the target to detector (**141**) is passed through a narrowband spectral filter set (**155**) to produce multiple detector regions, each sensitive to a different waveband wavelength range, and the detected light is spectrally analyzed to determine a measure of hydration, such as fluid losses, fluid ingested, fluid balance, or rate of fluid loss, in part based on a noninvasive measure of components of the bloodstream. In one example, variations in components of the bloodstream over time such as hemoglobin and water are determined based on the detected light, and the measure of hydration is then determined based on the in components of the bloodstream over time. In the absence of the LED light, ambient light may be sufficient illumination for analysis. The same sensor can provide identifying features of type or status of a tissue target, such as heart rate or heart rate variability, respiratory status, or even confirmation that the tissue is alive. Hydration monitoring systems incorporating the sensor, as well as methods, are also disclosed.

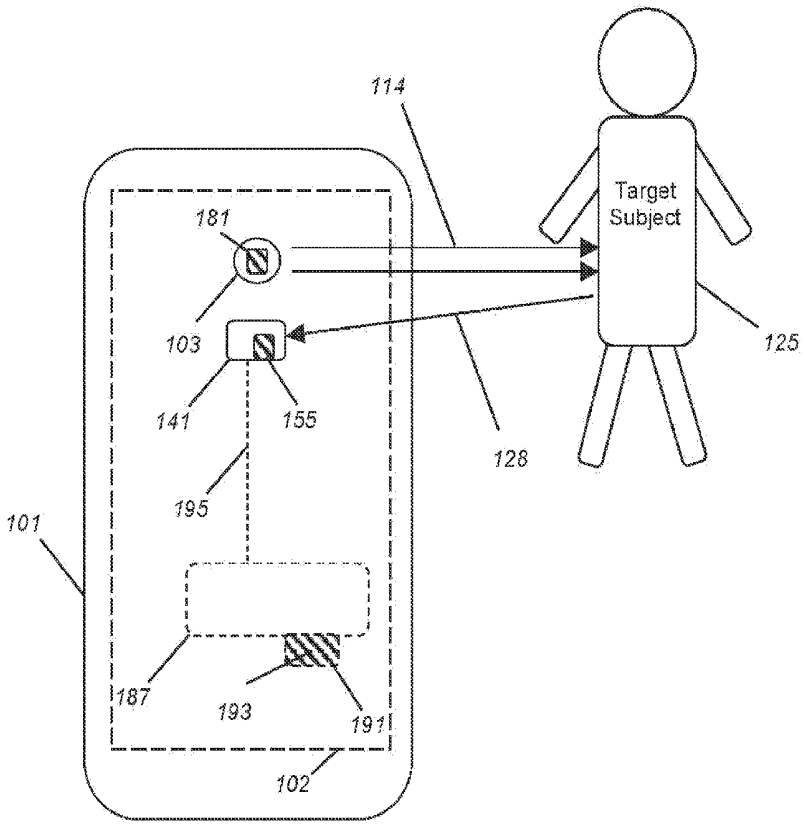

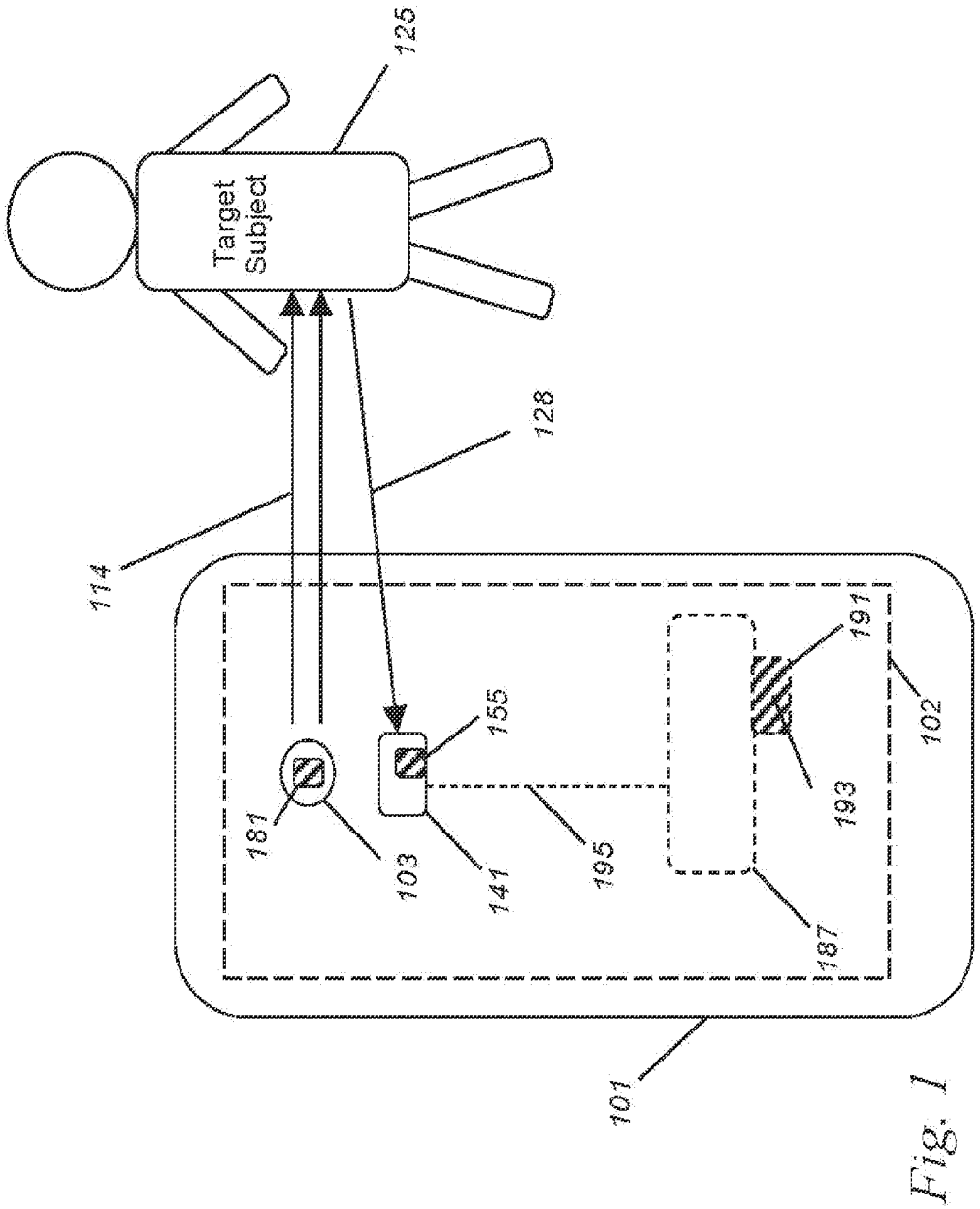
Target Subject
125
128
114
155
181
103
141
195
191
193
102
187
101

Fig. 1

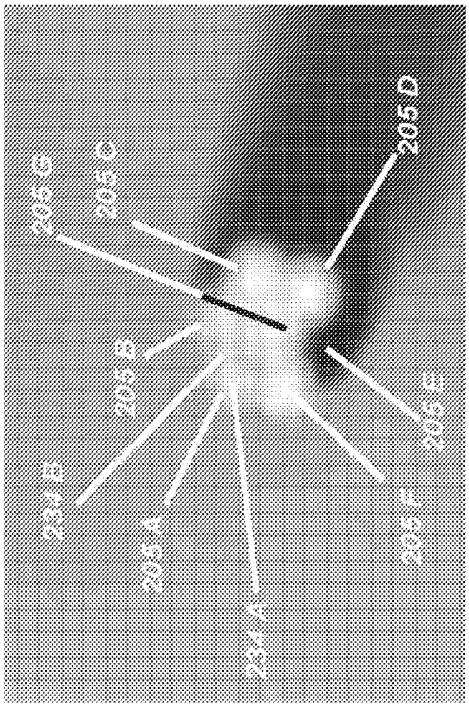
205 G
205 C
205 D
205 B
205 A
205 F
205 E
234 A

Fig. 2B

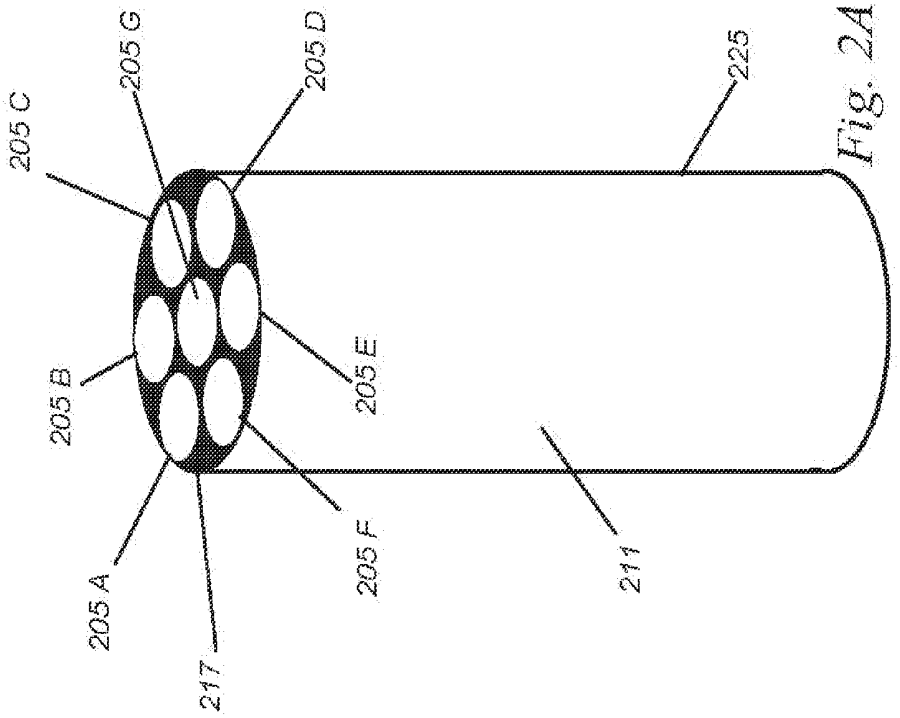
205 C
205 G
205 D
225
205 B
205 E
205 A
205 F
211
217

Fig. 2A

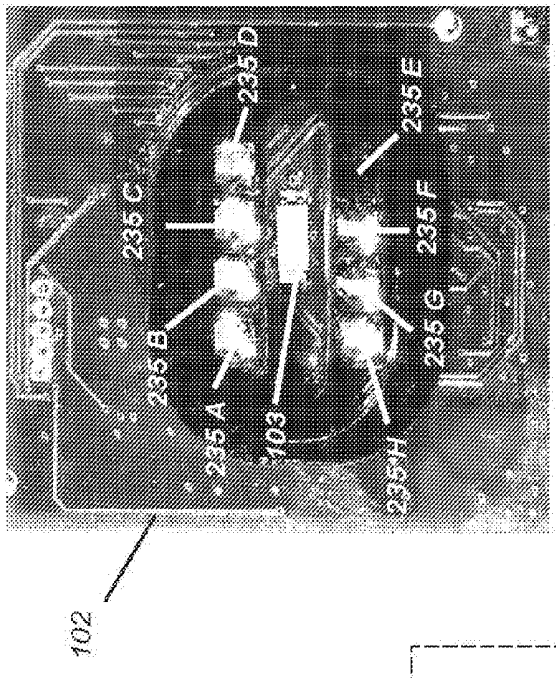
235 D
235 E
235 C
235 F
235 G
235 B
235 A
103
235 H
102

Fig. 2D

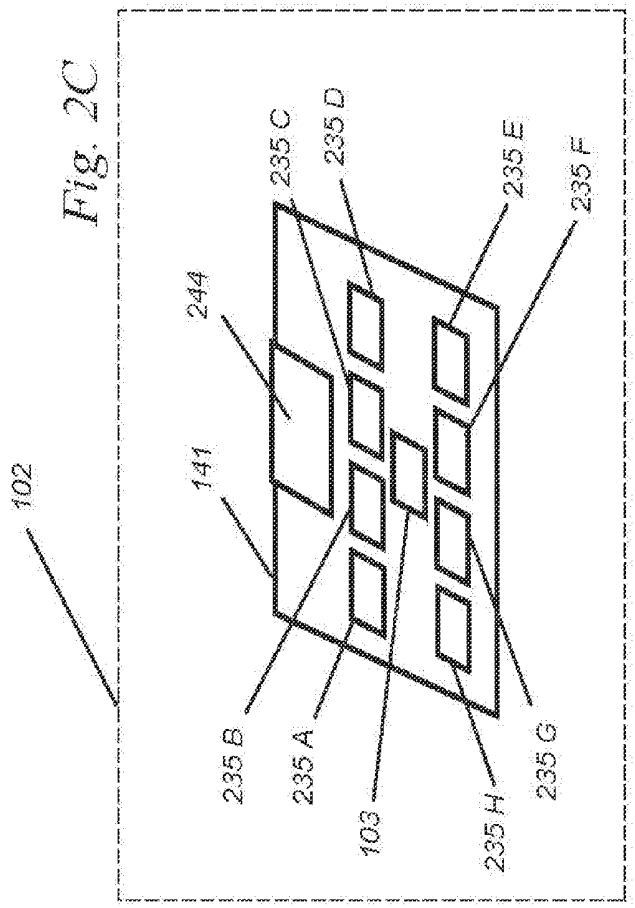
102
244
141
235 C
235 D
235 E
235 F
235 B
235 A
103
235 H
235 G

Fig. 2C

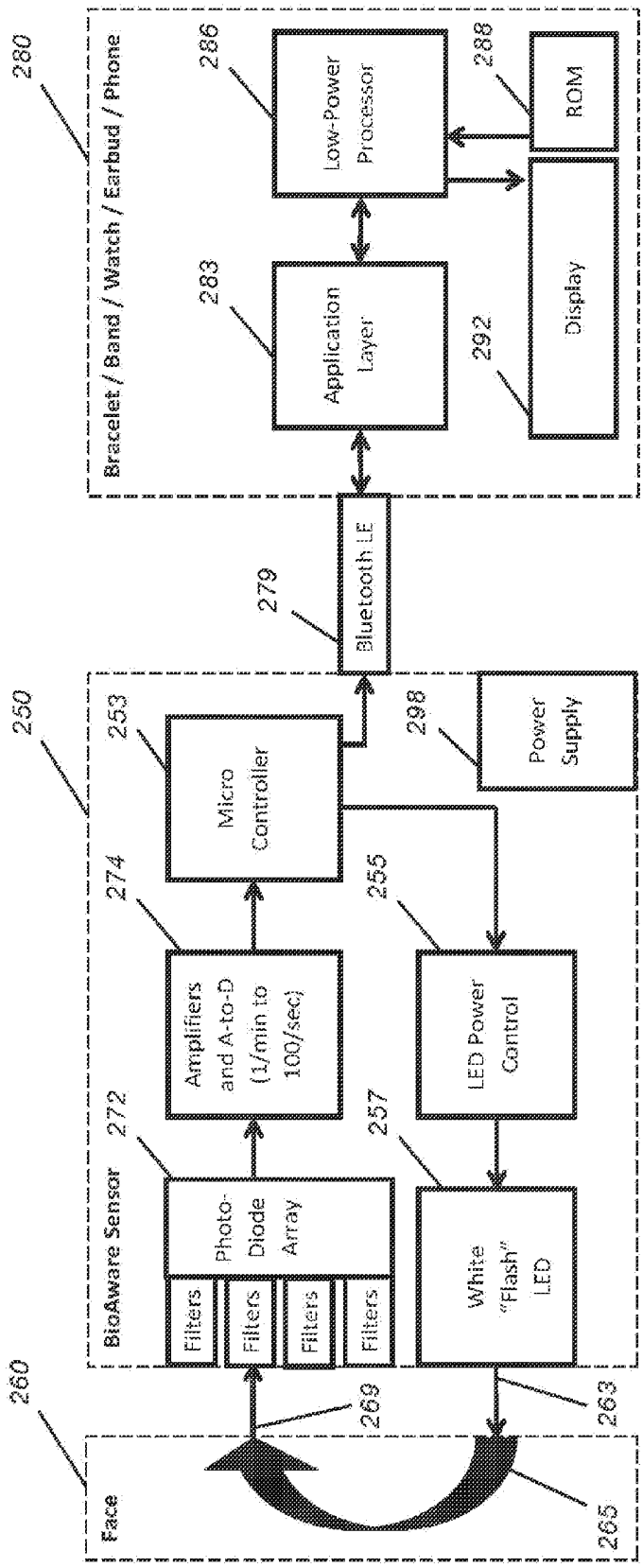
280
Bracelet / Band / Watch / Earbud / Phone
286
Low-Power Processor
288
ROM
283
Application Layer
292
Display
279
Bluetooth LE
250
253
Micro Controller
298
Power Supply
274
Amplifiers and A-to-D (1/min to 100/sec)
255
LED Power Control
BioAware Sensor
272
Photo-Diode Array
Filters
Filters
Filters
Filters
257
White "Flash" LED
260
269
263
Face
265

Fig. 2E

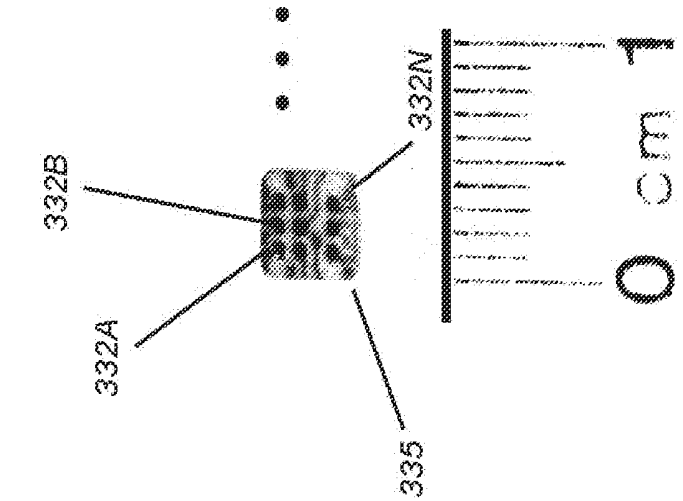

Fig. 3B

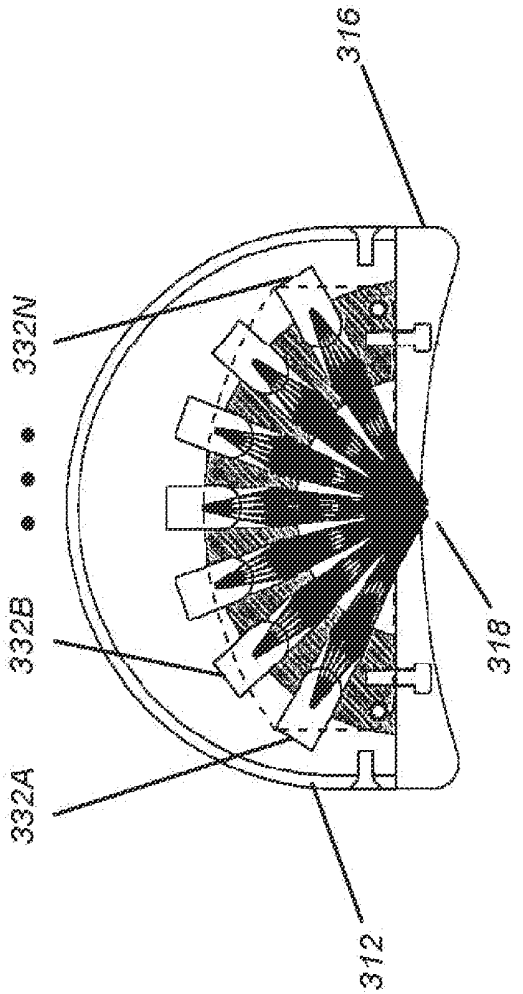

Fig. 3A

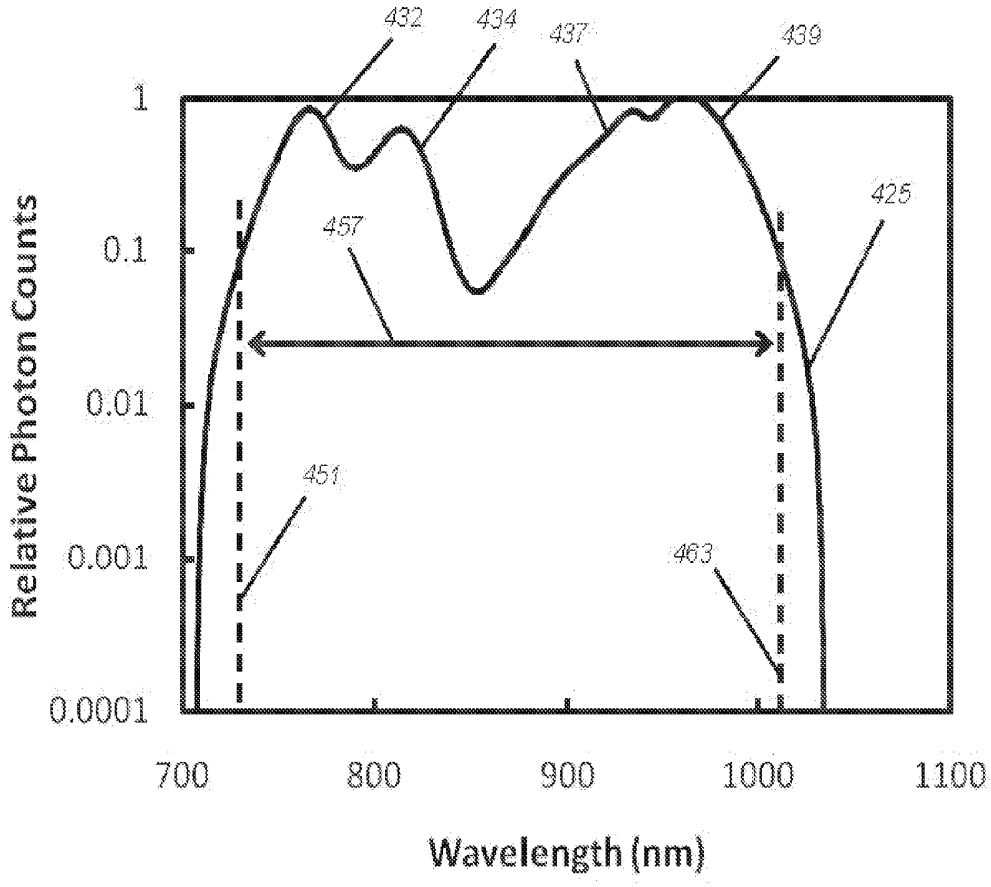
432
434
437
439
425
457
451
463
1
0.1
0.01
0.001
0.0001
Relative Photon Counts
700
800
900
1000
1100
Wavelength (nm)

Fig. 4

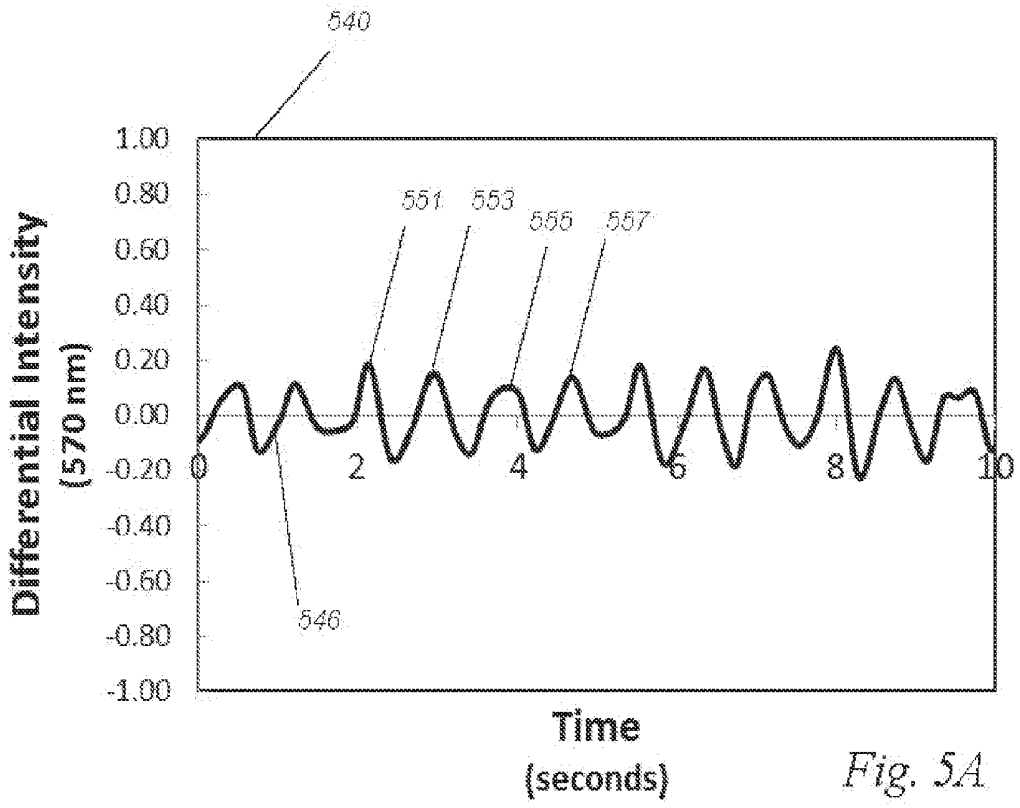
540
1.00
0.80
0.60
0.40
0.20
0.00
-0.20
-0.40
-0.60
-0.80
-1.00
Differential Intensity
(570 nm)
551
553
555
557
546
0
2
4
6
8
10
Time
(seconds)

Fig. 5A

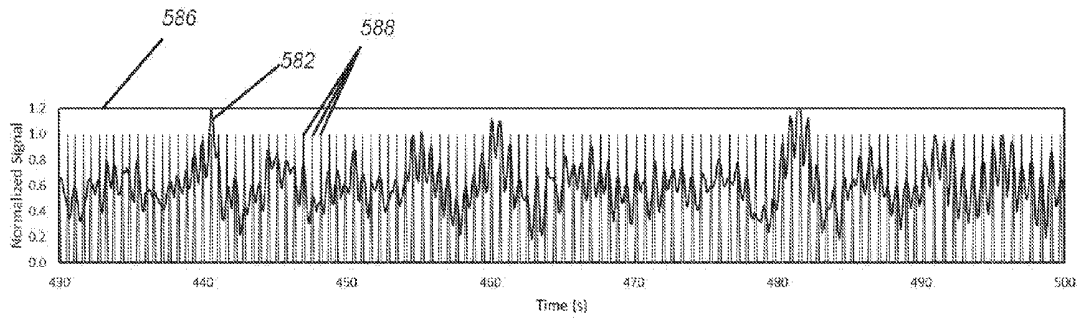
586
582
588
Normalized Signal
1.2
1.0
0.8
0.6
0.4
0.2
0.0
430
440
450
460
470
480
490
500
Time (s)

Fig. 5B

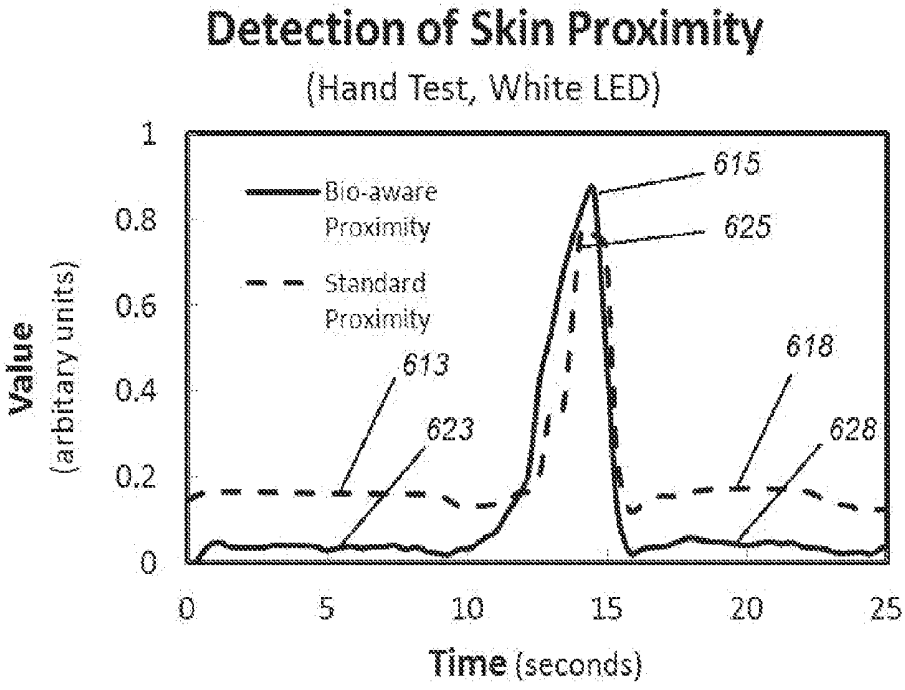
Detection of Skin Proximity
(Hand Test, White LED)
Value
(arbitary units)
1
0.8
0.6
0.4
0.2
0
Bio-aware Proximity
Standard Proximity
615
625
618
628
613
623
0
5
10
15
20
25
Time (seconds)

Fig. 6A

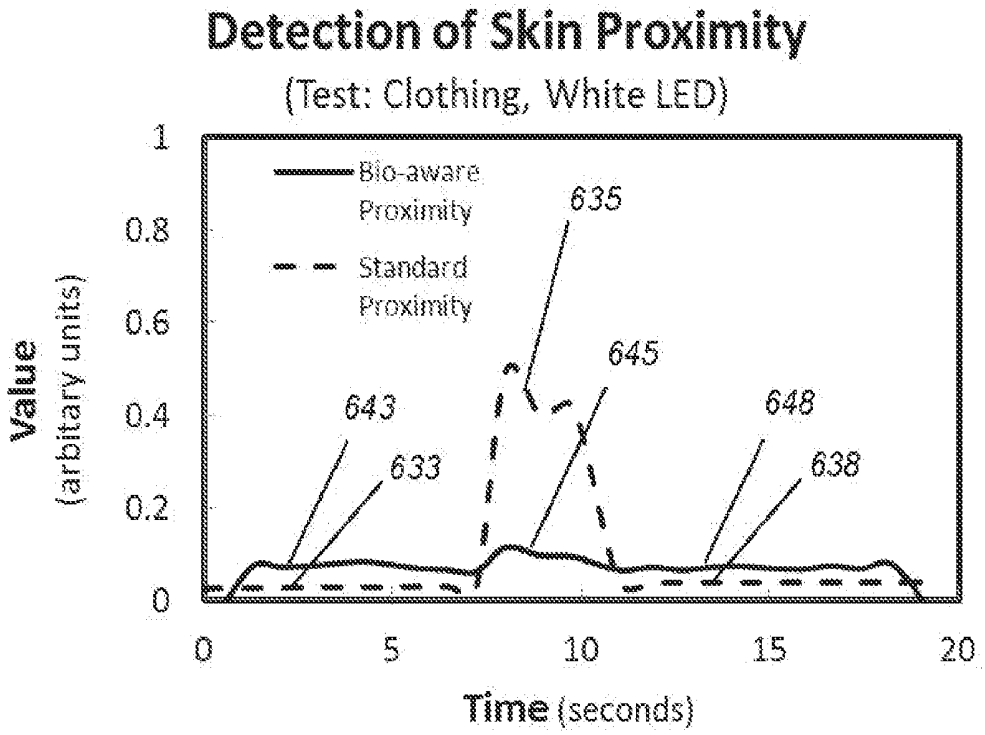
Detection of Skin Proximity
(Test: Clothing, White LED)
Value
(arbitary units)
1
0.8
0.6
0.4
0.2
0
Bio-aware Proximity
Standard Proximity
635
645
643
633
648
638
0
5
10
15
20
Time (seconds)

Fig. 6B

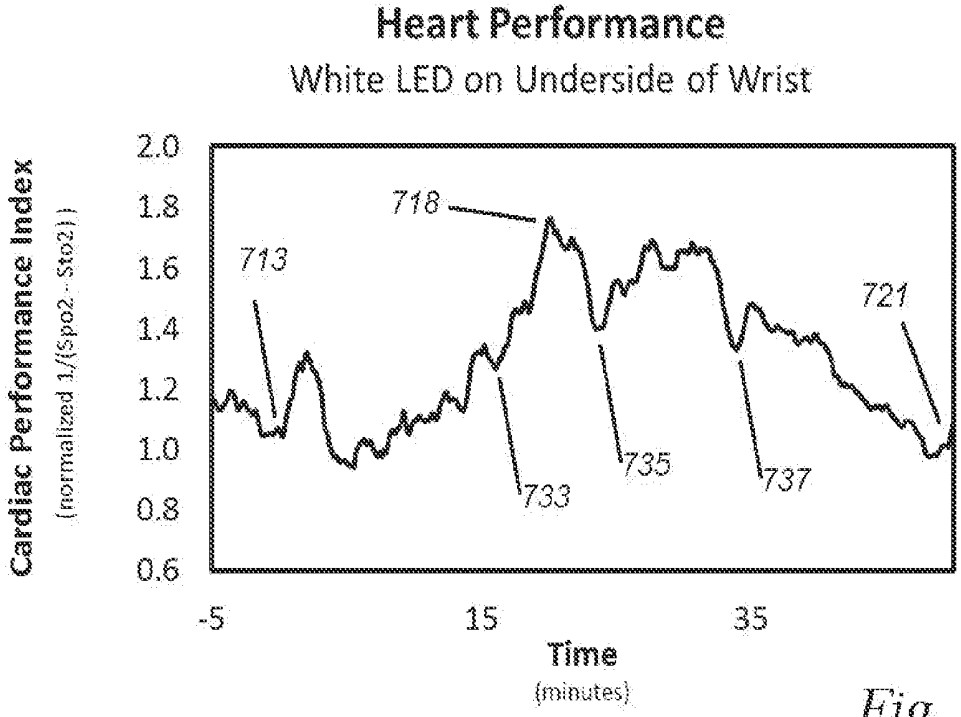
Heart Performance
White LED on Underside of Wrist
Cardiac Performance Index
(normalized 1/(Spo2 - Sto2))
2.0
1.8
1.6
1.4
1.2
1.0
0.8
0.6
718
713
721
733
735
737
-5
15
35
Time
(minutes)

Fig. 7

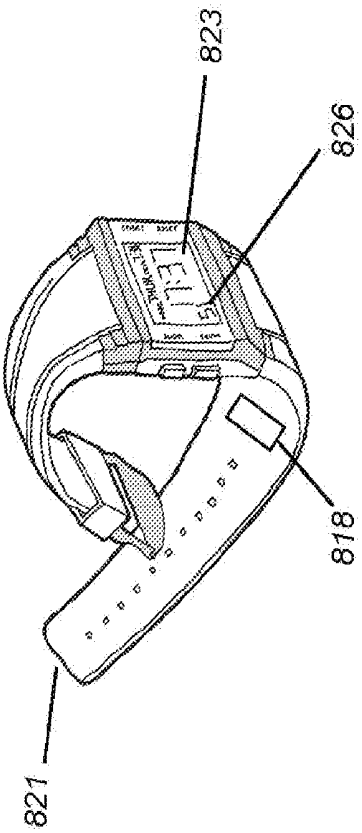

Fig. 8B

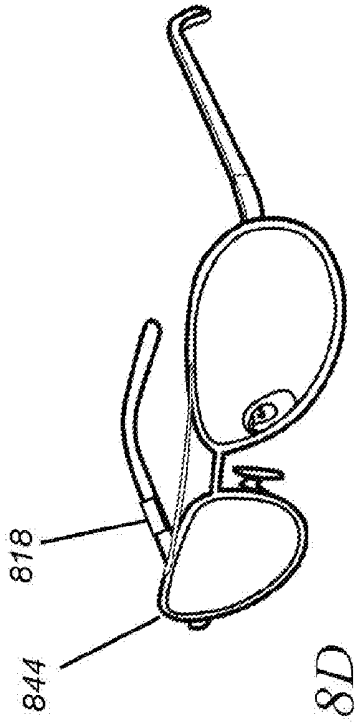

Fig. 8D

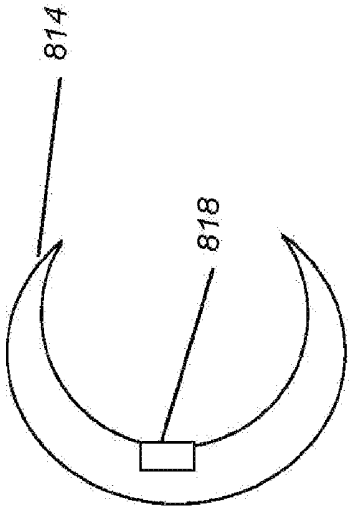

Fig. 8A

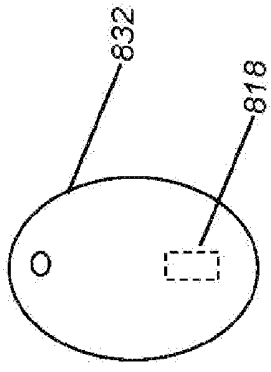

Fig. 8C

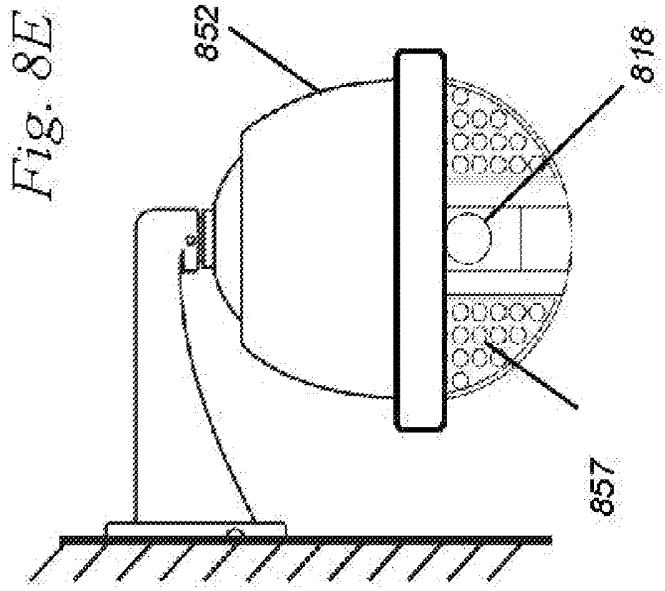

Fig. 8E

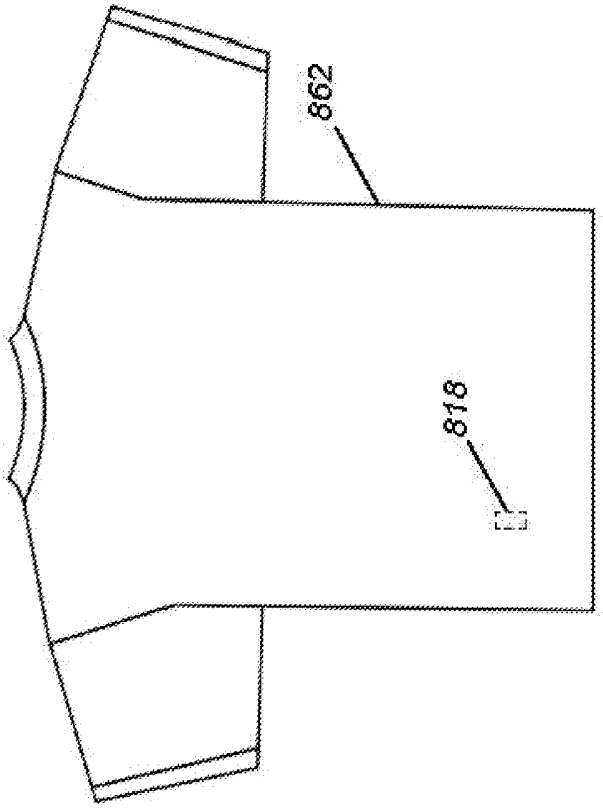

Fig. 8F

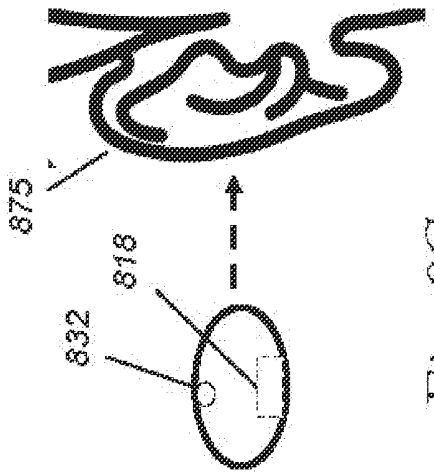

Fig. 8G

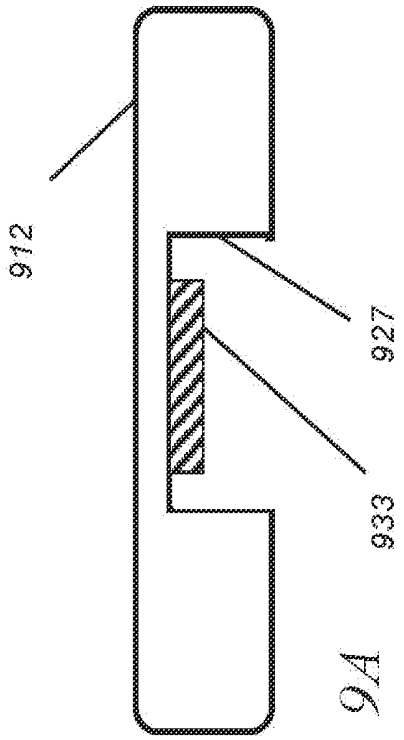

Fig. 9A

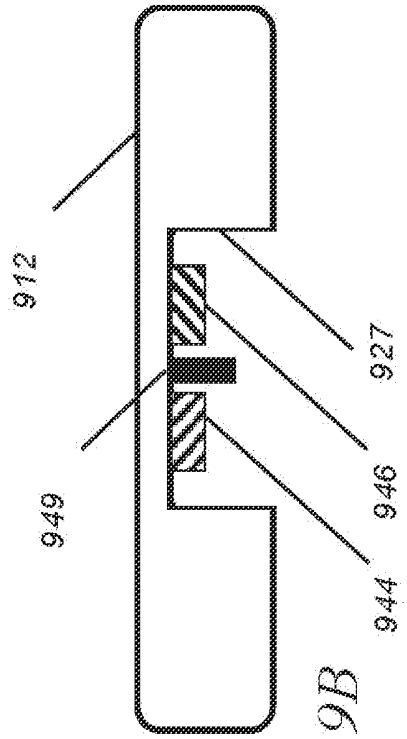

Fig. 9B

Fig. 10A

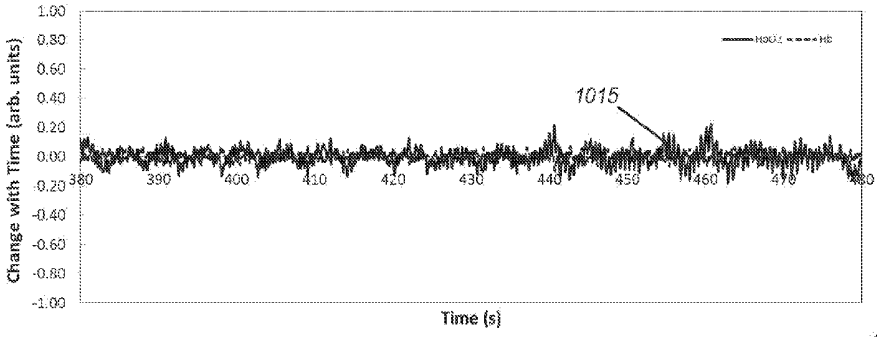

Fig. 10B

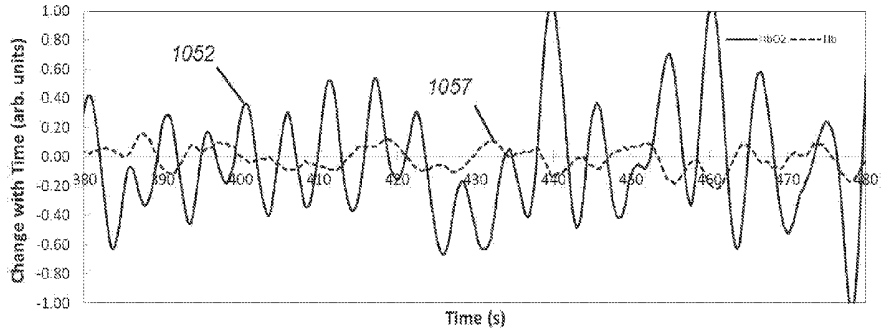

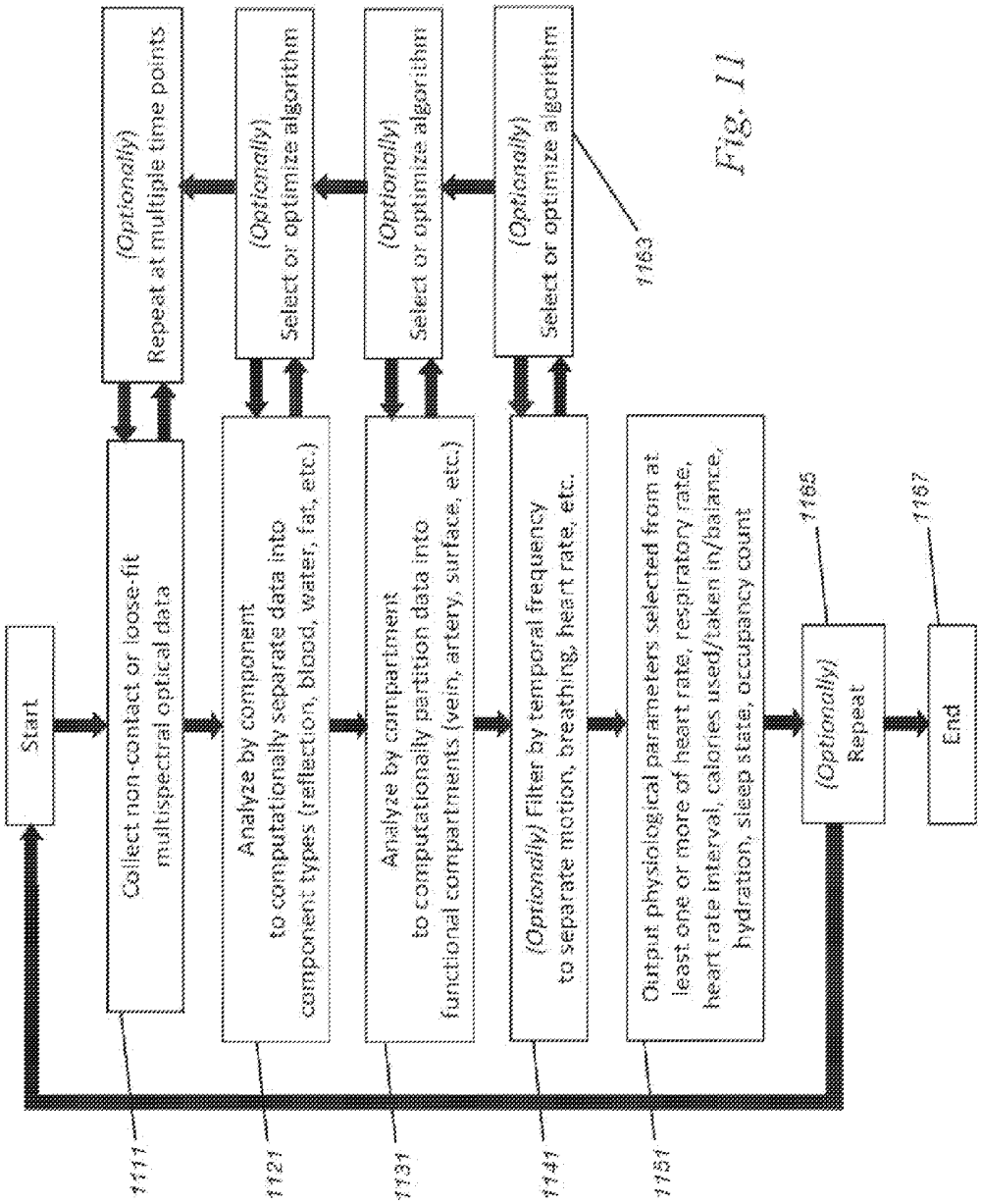
Start
Collect non-contact or loose-fit multispectral optical data
Analyze by component to computationally separate data into component types (reflection, blood, water, fat, etc.)
Analyze by compartment to computationally partition data into functional compartments (vein, artery, surface, etc.)
(Optionally) Filter by temporal frequency to separate motion, breathing, heart rate, etc.
Output physiological parameters selected from at least one or more of heart rate, respiratory rate, heart rate interval, calories used/taken in/balance, hydration, sleep state, occupancy count
(Optionally) Repeat
End
(Optionally) Repeat at multiple time points
(Optionally) Select or optimize algorithm
(Optionally) Select or optimize algorithm
(Optionally) Select or optimize algorithm
1111
1121
1131
1141
1151
1163
1165
1167

Fig. 11

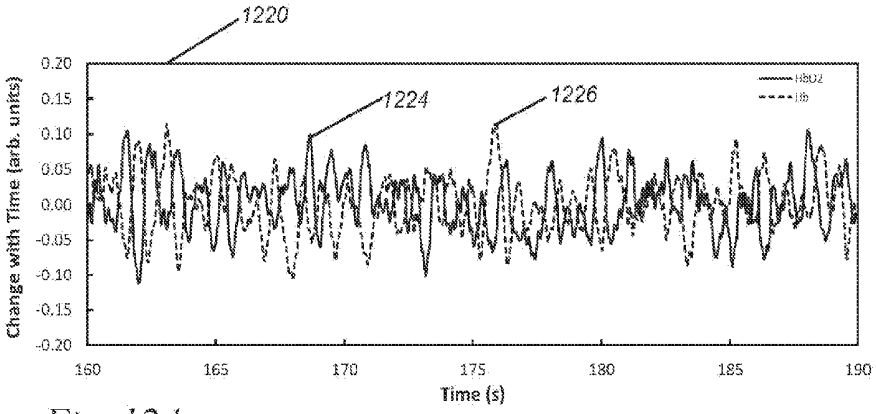

Fig. 12A

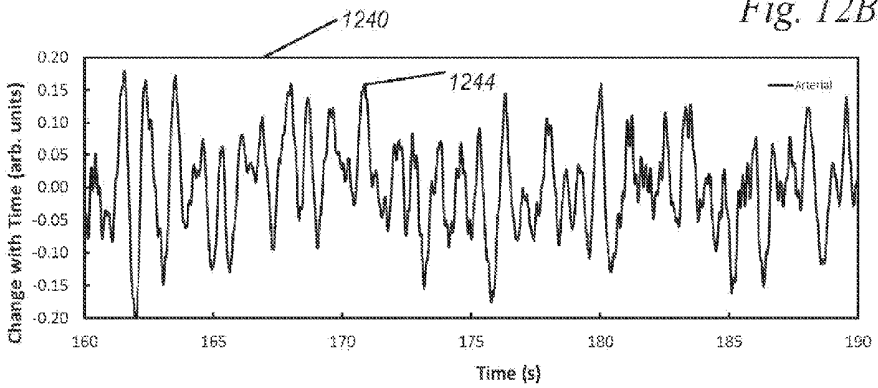

Fig. 12B

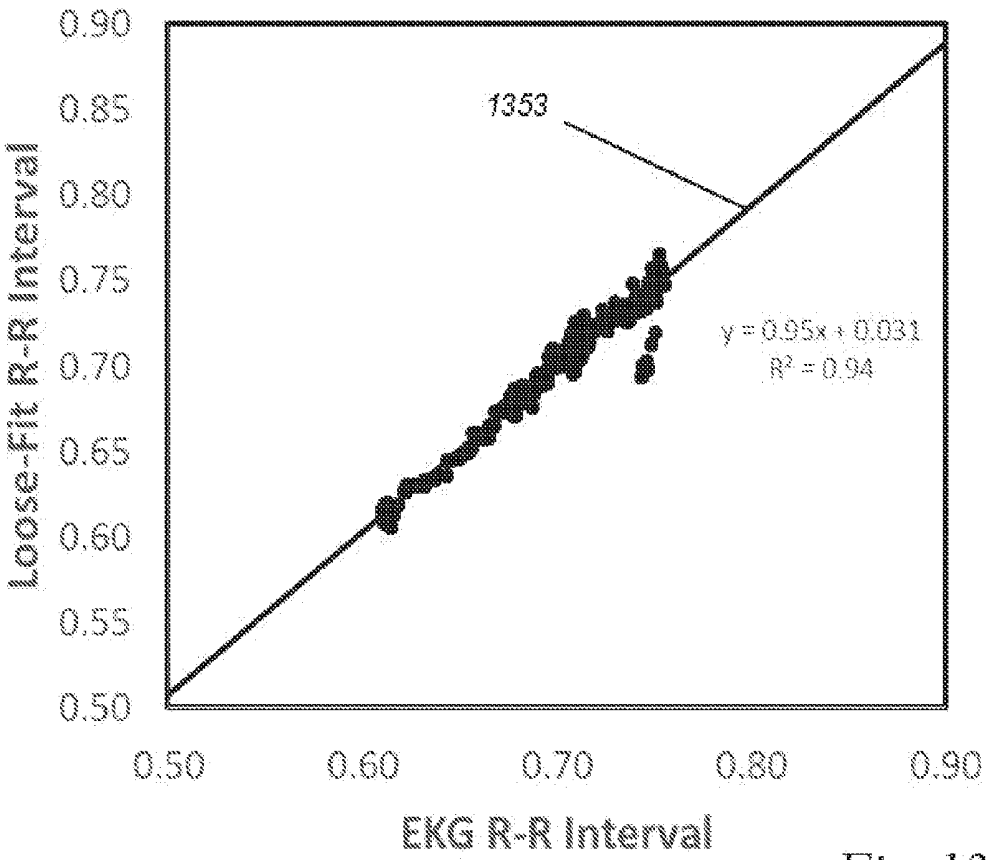
0.90
0.85
0.80
0.75
0.70
0.65
0.60
0.55
0.50
Loose-Fit R-R Interval
1353
y = 0.95x + 0.031
R² = 0.94
0.50
0.60
0.70
0.80
0.90
EKG R-R Interval

Fig. 13

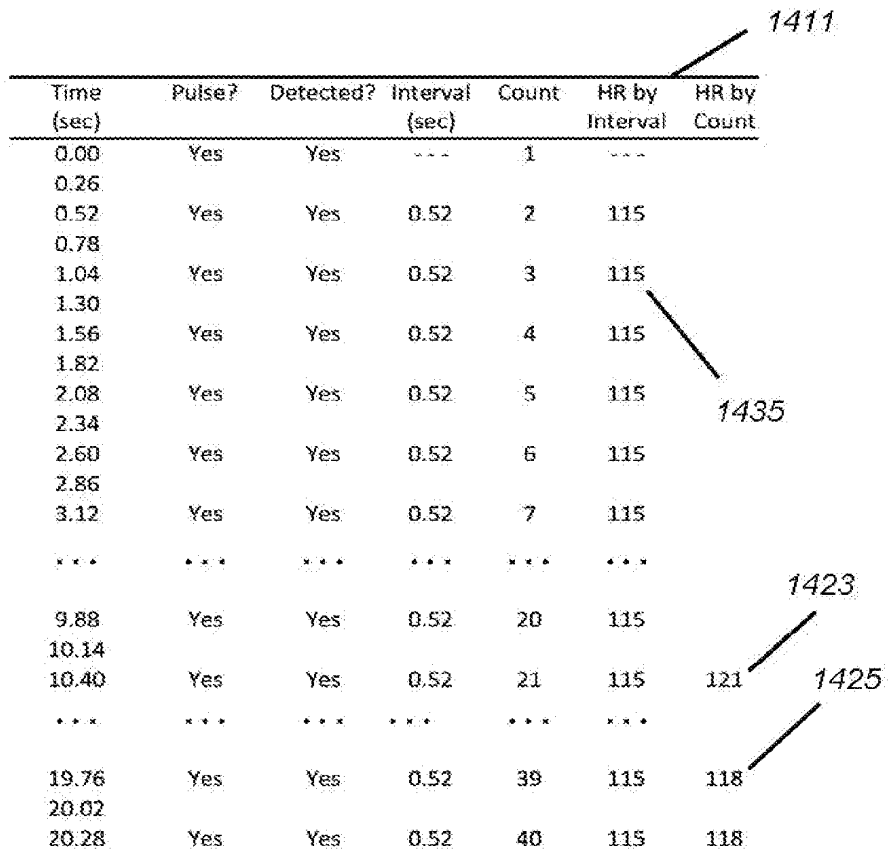

Time (sec)	Pulse?	Detected?	Interval (sec)	Count	HR by Interval	HR by Count
0.00	Yes	Yes	---	1	---	
0.26						
0.52	Yes	Yes	0.52	2	115	
0.78						
1.04	Yes	Yes	0.52	3	115	
1.30						
1.56	Yes	Yes	0.52	4	115	
1.82						
2.08	Yes	Yes	0.52	5	115	
2.34						
2.60	Yes	Yes	0.52	6	115	
2.86						
3.12	Yes	Yes	0.52	7	115	
...	...	...	...	...	...	
9.88	Yes	Yes	0.52	20	115	
10.14						
10.40	Yes	Yes	0.52	21	115	121
...	...	...	...	...	...	
19.76	Yes	Yes	0.52	39	115	118
20.02						
20.28	Yes	Yes	0.52	40	115	118

Fig. 14A

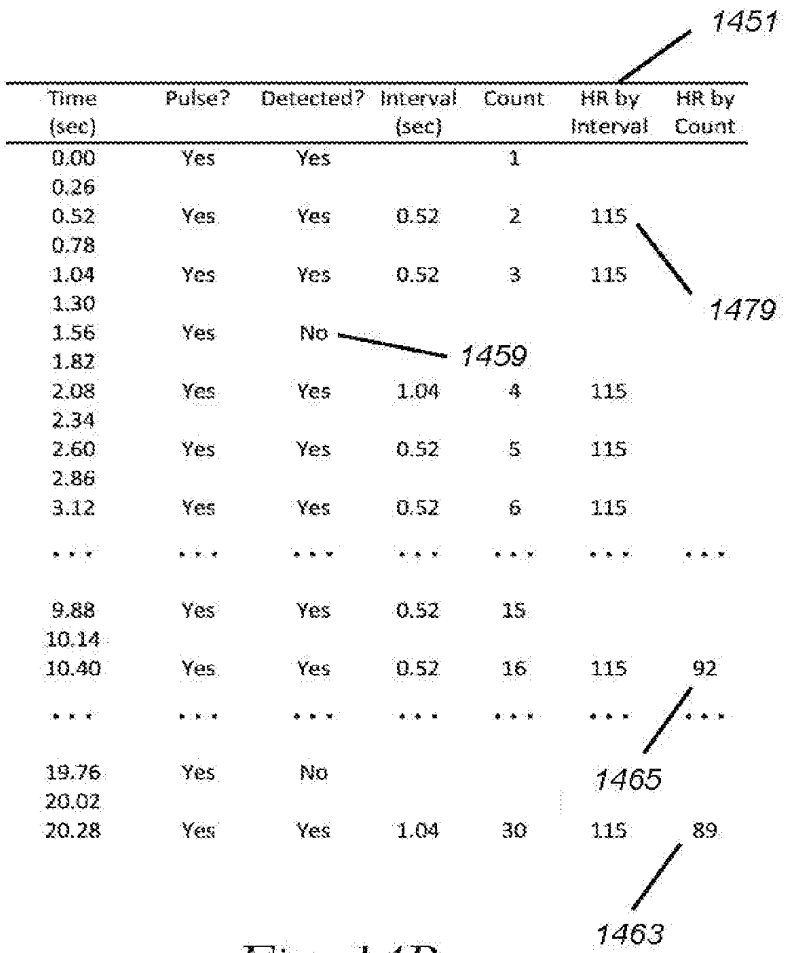

Time (sec)	Pulse?	Detected?	Interval (sec)	Count	HR by Interval	HR by Count
0.00	Yes	Yes		1		
0.26						
0.52	Yes	Yes	0.52	2	115	
0.78						
1.04	Yes	Yes	0.52	3	115	
1.30						
1.56	Yes	No				
1.82						
2.08	Yes	Yes	1.04	4	115	
2.34						
2.60	Yes	Yes	0.52	5	115	
2.86						
3.12	Yes	Yes	0.52	6	115	
...	...	...	...	...	...	...
9.88	Yes	Yes	0.52	15		
10.14						
10.40	Yes	Yes	0.52	16	115	92
...	...	...	...	...	...	...
19.76	Yes	No				
20.02						
20.28	Yes	Yes	1.04	30	115	89

Fig. 14B

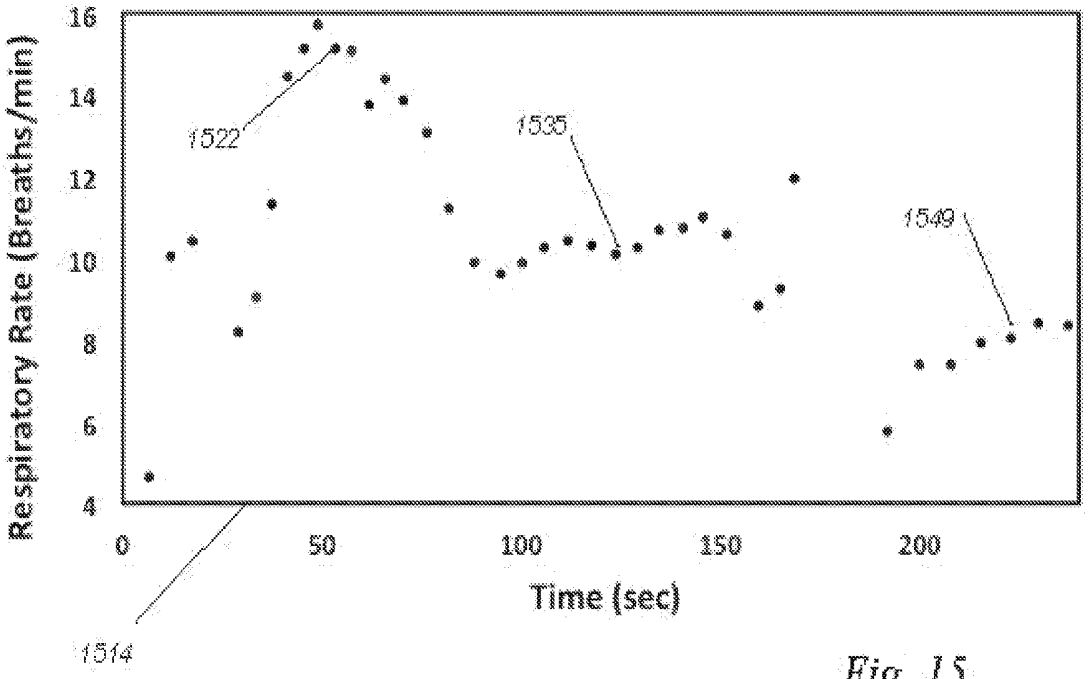
Respiratory Rate (Breaths/min)
16
14
12
10
8
6
4
0
50
100
150
200
Time (sec)
1522
1535
1549
1514

Fig. 15

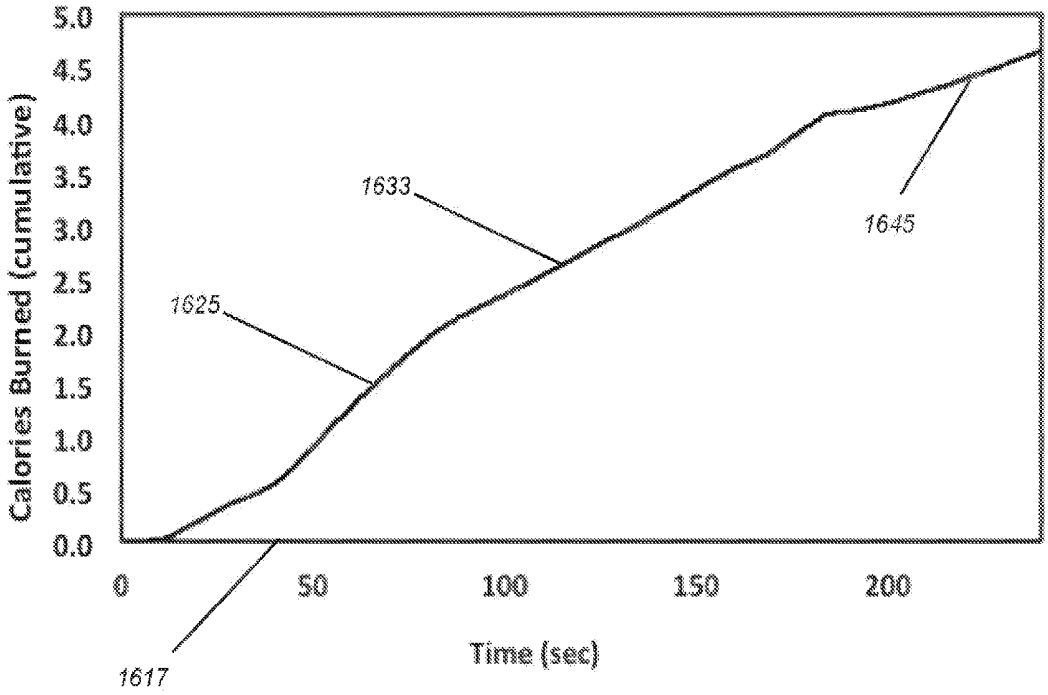
Calories Burned (cumulative)
5.0
4.5
4.0
3.5
3.0
2.5
2.0
1.5
1.0
0.5
0.0
0
50
100
150
200
Time (sec)
1617
1625
1633
1645

Fig. 16

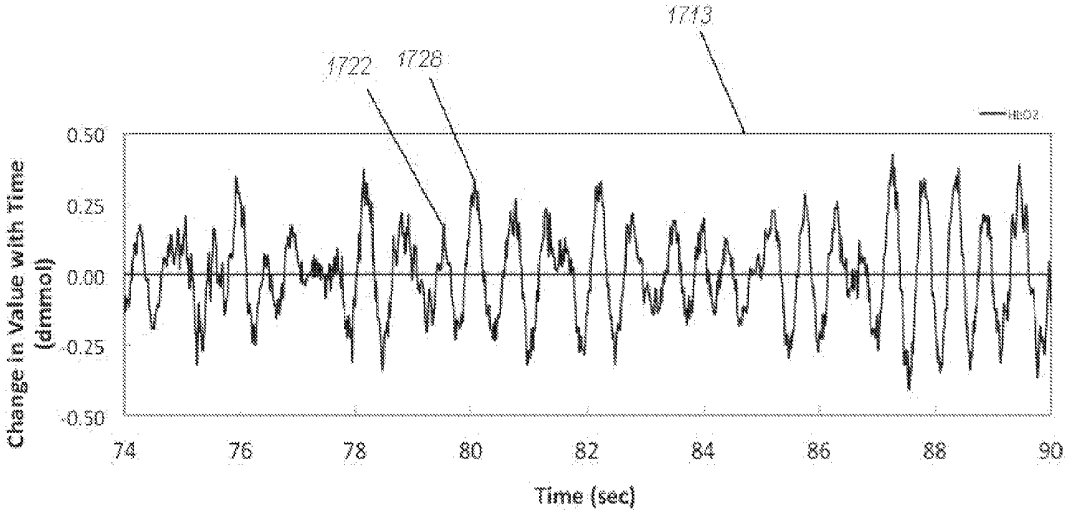
1713
1722
1728
0.50
0.25
0.00
-0.25
-0.50
Change in Value with Time (dmmol)
74
76
78
80
82
84
86
88
90
Time (sec)

Fig. 17

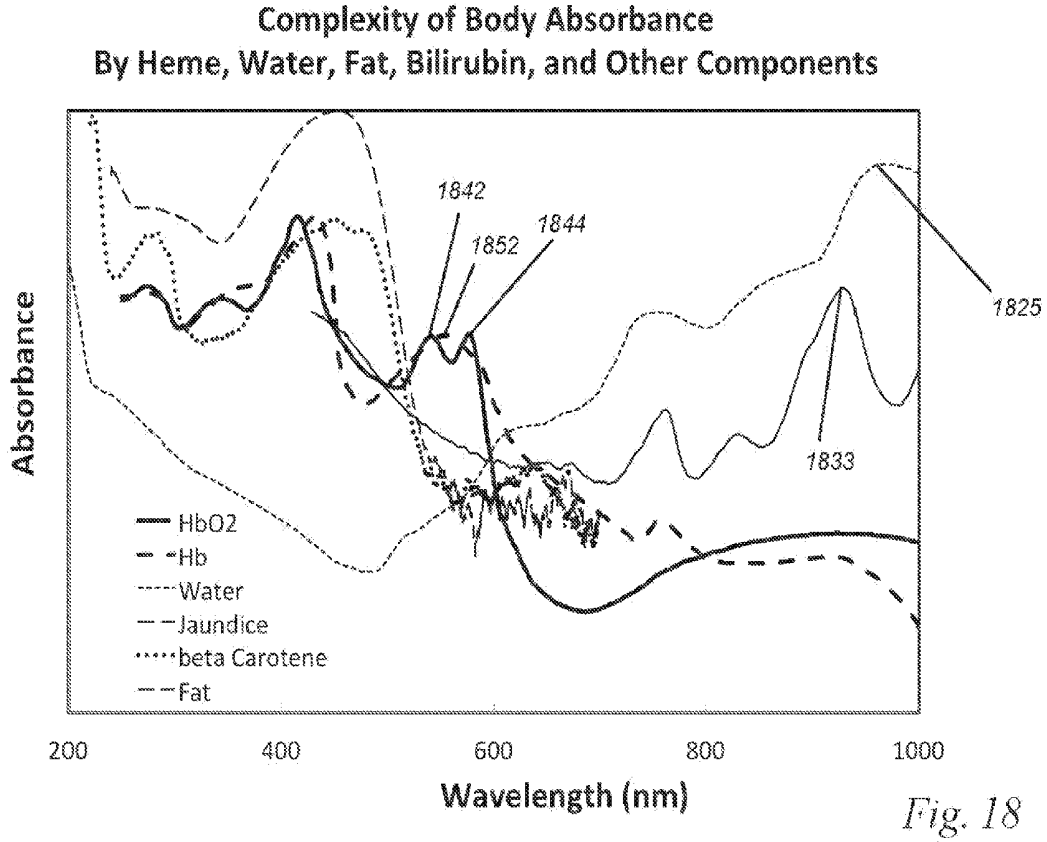
Complexity of Body Absorbance
By Heme, Water, Fat, Bilirubin, and Other Components
Absorbance
1842
1852
1844
1825
1833
HbO2
Hb
Water
Jaundice
beta Carotene
Fat
200
400
600
800
1000
Wavelength (nm)

Fig. 18

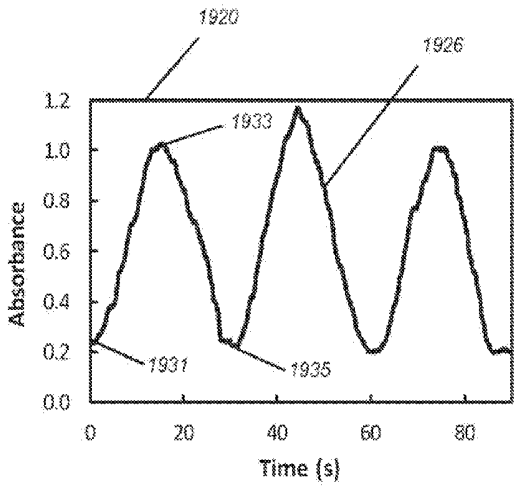

Fig. 19A

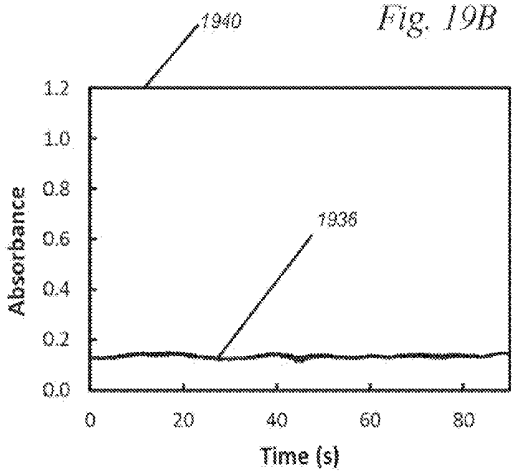

Fig. 19B

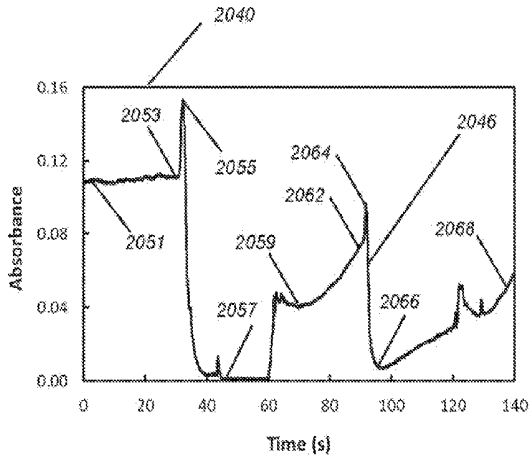

Fig. 20A

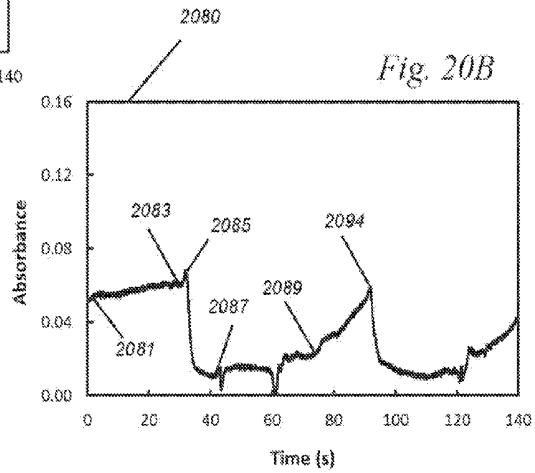

Fig. 20B

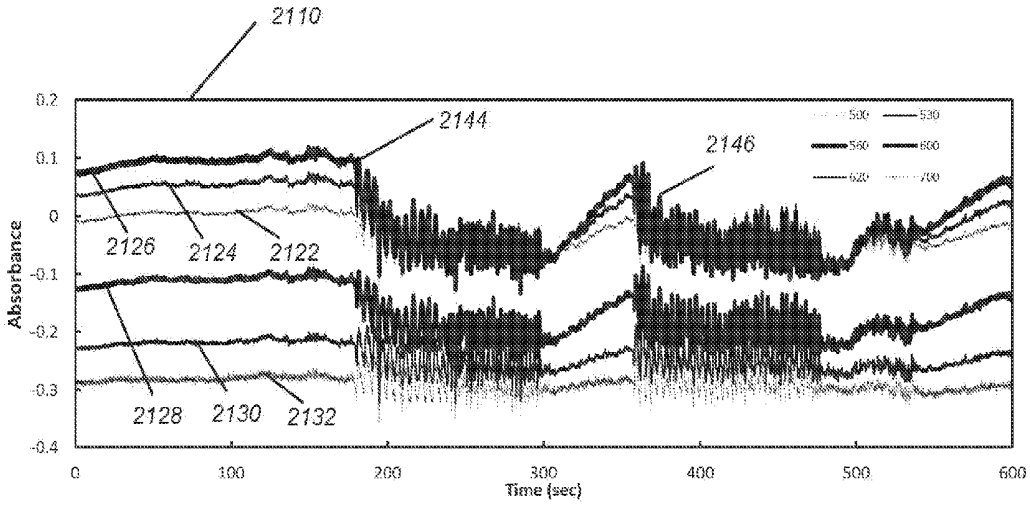
2110
2144
2146
2126
2124
2122
2128
2130
2132
Absorbance
Time (sec)
0.2
0.1
0
-0.1
-0.2
-0.3
-0.4
0
100
200
300
400
500
600

Fig. 21

HYDRATION MONITORING SENSOR AND METHOD FOR CELL PHONES, SMART WATCHES, OCCUPANCY SENSORS, AND WEARABLES

CROSS-REFERENCES TO RELATED APPLICATIONS

[0001] This application claims the benefit of, and priority to, U.S. Provisional Pat. Appn. No. 61/908,926, filed Nov. 26, 2013, U.S. Provisional Pat. Appn. No. 61/970,667, filed Mar. 26, 2014, and U.S. Provisional Pat. Appn. No. 61/989,140, filed May 6, 2014, U.S. Provisional Pat. Appn. No. 62/050,828, filed Sep. 16, 2014, U.S. Provisional Pat. Appn. No. 62/050,900, filed Sep. 16, 2014, U.S. Provisional Pat. Appn. No. 62/050,954, filed Sep. 16, 2014, U.S. Provisional Pat. Appn. No. 62/053,780, filed Sep. 22, 2014, U.S. Provisional Pat. Appn. No. 62/054,873, filed Sep. 24, 2014, the entire contents of each of which is incorporated herein in their entirety by this reference.

FIELD OF THE INVENTION

[0002] The present invention relates generally to a hydration-sensing wearable device and method using light. More particularly, embodiments provide a narrowband-filter coated multi-element photodiode sensor for determining a hydration measurement in a living subject using spectral analysis of variations in water and/or hemoglobin content of the bloodstream detected noninvasively using broadband light from ambient sunlight, ambient room light, or light from a solid-state broadband white LED. Enabling systems and methods for incorporating or practicing the improved hydration sensing are also disclosed

BACKGROUND OF THE INVENTION

[0003] The traditional input for a consumer hydration monitoring device is a notebook or diary application running on a watch or smartphone, into which the subject user enters a record of when, what, and how much of a drink is consumed. This can be part of a calorie-tracking diary that also tracks food consumption. These can be augmented by accelerometers or gyros, or a GPS signal that determine how much the body has physically moved, which is correlated with hydration losses. In these cases, a certain distance travelled over a certain terrain in a certain way can be translated to an estimate of the water losses expended. Other sensors can be added, such as chemical sensors to detect surface sweat.

[0004] What is common to these traditional physical approaches is that they are dependent on the physical action, but that they are insensitive to what the body is actually doing. For example, if we do not move, most of us still burn over 1,000 Calories in a day and require fluids. By weight, the average 70 kg subject needs about 2.5 liters of water at rest, and this can increase several fold when exercise is added. This is due to a basal metabolic rate, respiratory losses, and the need to generate urine to remove circulating products of metabolism, as well as other reasons. However, a physical motion sensor yields an incomplete picture. An algorithm using an accelerometer can correct for a minimum basal rate, but it is a correction . . . there is no physical motion sensed. Similarly, if we have a fever, we burn calories and use fluids more quickly. However, an accelerometer or GPS based calorie sensor will not detect this. Further, weight lifting using a limb other than the one monitored by an accelerometer, or stationary cycling with a sensor one a non-moving wrist, fidgeting with one's feet, and other normal movements all affect calories expended, but are not detected by the traditional sensor.

[0005] Heart rate does change with exercise, and can be used to estimate water losses as well, but heart rate is affected by blood flow not related to energy consumption, such as blood to the skin to cool the body on a hot day, or blood to the kidneys to increase urine flow. Thus, heart rate is not a direct measure of water requirements or water status.

[0006] In the laboratory, the amount of water lost, even at rest, can be measured in the breath, urine, stool, and skin surface water sensors, but such devices are typically cumbersome, requiring delivery of air with in system analyzers unlikely to have appeal to the average mass consumer. Such a system would be difficult to use in the subject is ambulatory or exercising. In the end, however, it really should not matter if water is lost on a stationary cycle or during the Tour de France, the user should be able to estimate water losses and water status.

[0007] Similarly, a user would like to know water taken in via meals and fluids, without having to record the mass of the food or the volume of fluids ingested, and entering this data into a database. Accelerometers could record hand to mouth movement, and this can identify the last time food or water has been ingested, but typically consumer devices miss this important task of eating and drinking Detecting water ingested would allow for a better determination of fluid balance.

[0008] Thus, conventional hydration monitoring mobile and wearable systems and methods suffer from one or more limitations noted above, in that they are not for mass consumer use, are difficult to use, rely on accelerometers or GPS for movement-based estimates, and therefore do not measure actual losses and miss stationary expenditures, ignore fluid intake, and/or they ignore or omit design considerations regarding optimizing fluid or hydration monitoring in living beings and tissues.

[0009] None of the above systems suggest or teach a method and system using light to estimate fluid losses, intake, balance, or rate of fluid loss in a manner that is responsive to physiology, including detecting basal fluid losses as well as losses not related to motion. Nor do the above systems teach estimation of fluid intake using light. More specifically, none of the above systems suggest or teach a method and system to monitor fluid balance in tissue or the bloodstream, or other optical signatures associated with fluid balance. And none of the above systems work well for continuous monitoring of resting, ambulatory, or exercising subjects. Such a device for real-time sensing applications has not been taught, nor has such a tool been successfully commercialized.

SUMMARY AND OBJECTS OF THE INVENTION

[0010] The present invention relies upon the discovery that certain features of physiology correlate with hydration status, and with the right measures, one can estimate fluid expenditures, intake, balance, and rate of losses. Similarly, such measures can be made to estimate fluid ingestion, allowing implementation more simply and inexpensively than has been achieved in a similar device and/or configuration using conventional approaches. Such discovery led to development of

a new sensor, allowing implementation more simply and inexpensively than has been achieved using conventional approaches.

[0011] A salient feature of the present invention is that mobile sensors and illuminators can detect chemical signatures (water absorbance, water to heme ratios in tissue, capillary perfusion adequacy), and that these measures can be correlated with hydration status such that fluid balance, physiology and exercise hydration monitoring, and even fluid ingestion monitoring can be beneficially enabled.

[0012] Another salient feature is that tissue water can be monitored, at the sensor level, using light, at a low or reduced cost, enabling fluid intake monitoring as well as fluid loss monitoring.

[0013] Another feature is that these determinations are useful over time, integrating the measures to yield a story over days, weeks, months, or years.

[0014] Another feature is that physiology, such as heart rate, respiratory rate, heart rate interval, calories, arterial oxygenation, and tissue oxygenation can be extracted from these measures.

[0015] A final salient feature is recognition that such devices can be incorporated into many devices, including phones, watches, wristbands, pendants, traffic lights, street monitors, glasses, and the like. The device can be embedded in clothing (caps, belts, pants, sweats, shirts, suits), both for casual, work, and even professional use such as firefighters, police, pilots, and soldiers.

[0016] Accordingly, an object of the present invention is to provide a hydration sensor, including hardware and processing, to allow sensing and detection of type or state in mobile and imaging systems.

[0017] Another object is to provide a method for the stable detection fluid lost or ingested, fluid balance, and rate of fluid lost.

[0018] Another object is to provide these measures non-invasively.

[0019] Another object is to provide a method for the stable detection of the certain transient features of material sensed or imaged, such as to detect a rate of fluid lost expended, heart rate, heart rate variability, respiratory rate, arterial oxygenation, and tissue oxygenation.

[0020] Another object is to provide a combination of a white or broadband LED, one or more spectral filters integrated with one or more optical sensors, and a processing layer into order to produce an integrated sensor/processor that provides a determination or result, such as hydration status, or proximity of a hand containing water, or even to measure other nearby bodies, such as to record the rates of water loss in all persons in a business meeting in non-contact imaging manner.

[0021] Another object is to provide a sensor for embedding into nearly any mobile device, such as into a smartphone, personal wearable items (bracelet, pendant, watch, smart glasses, smart earbuds) and even into wearable clothing (shoe, shirt, or pants).

[0022] Another object is to provide an inexpensive spectral filter suitable for mass production.

[0023] Another object is to provide an inexpensive broadband solid-state light source of a configurable wavelength range.

[0024] The improved hydration sensor for mobile use as described has multiple advantages.

[0025] One advantage is that this improved sensor may now be safely deployed within cell phones, smart watches, or sports bracelets, wherein use of conventional sensors would have provided less information, been less reliable, been more costly, or been less functional. This includes in autos (for example, a sensor that analyzes your heart rate and alcohol content as an image in a non-contact manner before starting), or a military helmet (analyzes heart rate of all troops in your view, to identify subjects are risk for failure), or fitness clothing (analysis heart performance during a race), or medical monitors (alerts your physician when your heart is no longer working optimally).

[0026] Another advantage is that the improved sensors can enable new types of monitoring, from reliable non-contact sports monitoring to remote healthcare monitoring to business meeting monitoring in which the reactions and heart rates of all participants is known.

[0027] A final advantage is that the improved sensor, by virtue of its content-awareness or bio-awareness, can be incorporated into new devices and applications.

[0028] There is provided a hydration sensor for cell phones, health devices, and wearables. In one example, the system uses a phosphor-coated white LED and photodiodes with spectral filters, a processor, and software, to produce a system that reports on hydration status, such as fluid expenditure, fluid ingestion, fluid balance, and rate of fluid loss, when worn on the hand or finger, arm, ankle, face, ear, or other parts of the body, even in clothing. Systems incorporating this sensor for physiological monitoring, gesture enabling, and signature verification, and methods of use, are also described.

[0029] The breadth of uses and advantages of the present invention are best understood by example, and by a detailed explanation of the workings of a constructed apparatus, now in operation and tested in model systems and on human volunteers. These and other advantages of the invention will become apparent when viewed in light of the accompanying drawings, examples, and detailed description.

BRIEF DESCRIPTION OF THE DRAWINGS

[0030] FIG. **1** is a schematic of an operating system using a cell phone and a small multispectral filter, constructed in accordance with the present invention.

[0031] FIG. **2**A shows a fiber bundle multispectral filter.

[0032] FIG. **2**B shows a photograph of a fiber bundle filter during testing.

[0033] FIG. **2**C shows a sensor chip using spectral coatings on glass placed on a silicon detector chip, with collimating tubes and filter and shaping optics over each detector.

[0034] FIG. **2**D shows a photograph of a sensor board built using coated spectral filters placed on silicon chip detectors constructed in accordance with the present invention.

[0035] FIG. **2**E shows a schematic of a single-chip sensor chip.

[0036] FIG. **3**A shows a broadband LED constructed from individual LEDs for use in the infrared.

[0037] FIG. **3**B shows a photograph of a broadband infrared LED source array.

[0038] FIG. **4** shows the optical spectrum measured from a broadband infrared LED constructed in accordance with the present invention.

[0039] FIG. **5**A shows a real-time, non-contact heart rate data stream, collected in this case 3-5 times a second from multispectral sensor in a cell phone constructed in accordance with the present invention.

[0040] FIG. **5**B shows a real-time, non-contact heart rate data stream, collected from a multispectral sensor focusing on blood in the arterial supply as compared to a chest-lead medical EKG.

[0041] FIG. **6**A shows data spectral data from a hand collected from a spectrally resolved sensor configured as a smart proximity detector to detect tissue, but not a book or a face.

[0042] FIG. **6**B shows data spectral data from an arm with a sleeve covering the wrist collected from a spectrally resolved sensor configured as a smart proximity detector to detect tissue, but not a book or a face

[0043] FIG. **7** shows data from a wrist-based based sensor during exercise showing heart performance.

[0044] FIG. **8**A shows a schematic side-view of a system incorporating the sensor into a loose-fit wristband.

[0045] FIG. **8**B shows a schematic view of a system incorporating the sensor into a wristwatch.

[0046] FIG. **8**C shows a system incorporating the sensor into a loose-fit non-contact pendant.

[0047] FIG. **8**D shows a system incorporating the sensor into wearable glasses.

[0048] FIG. **8**E shows a system incorporating the sensor into an energy-saving motion sensor for illumination control.

[0049] FIG. **8**F shows a system incorporating the sensor into clothing.

[0050] FIG. **8**G shows a system incorporating the sensor into an earphone earbud.

[0051] FIG. **9**A shows a recessed non-contract sensor with the illumination and detection on the same chip.

[0052] FIG. **9**B shows a non-contact recessed sensor where the white LED illuminator is separate from the detector.

[0053] FIG. **10**A-B show respiratory rate detected using the arterial signal size. FIG. **10**A shows loose fit oxy- and deoxy-hemoglobin data measured during exercise from a human subject over 100 seconds, with a filter with a time constant of 0.15 seconds, emphasizing the arterial pulse variations. FIG. **10**B shows the same data with a 2 second time constant, emphasizing the arterial respiratory variations.

[0054] FIG. **11** shows a schematic flow chart of an approach incorporating the method of the present invention

[0055] FIG. **12**A-B show data analyzed for oxygenation in accordance with the algorithm of the prior figure, and compartmentalized into venous and arterial compartments after both stabilization for skin changes, and differential analysis to emphasize changes over time. FIG. **12**A shows calculations for changes in oxy- and deoxy-hemoglobin. FIG. **12**B shows calculations resolved just to the arterial pulse compartment.

[0056] FIG. **13** shows using intervals to determine rate, in this case heart beat interval accuracy as determined by arterial compartment pulse and by EKG from data during exercise and movement, with a correlation coefficient of 0.94.

[0057] FIG. **14**A-B show model data of how interval-based and counting-based rate estimation differ. FIG. **14**A shows rate estimation in the presence of good data with no dropouts.

[0058] FIG. **14**B shows rate estimation in the presence of noise with some signal drop out.

[0059] FIG. **15** shows a plot of respiratory rate as measured and determined in accordance with the present invention on a human subject breathing at a controlled rate.

[0060] FIG. **16** shows cumulative calories expended as measured and calculated in accordance with the present invention on a human subject under study conditions.

[0061] FIG. **17** shows a multispectral signal detected using only ambient light.

[0062] FIG. **18** shows the selected components of a complex absorbance of hemoglobins, bilirubin, water, fat, and other substances.

[0063] FIG. **19**A-B show data collected during movement of the sensor compared to the subject. FIG. **19**A shows data during movement that obscures the heart rate effect by adding noise much larger than the signal. FIG. **19**B shows data during movement but corrected for the movement using multispectral analysis.

[0064] FIG. **20**A-B show data collected during movement of the subject but with a relatively stable sensor position. FIG. **20**A shows data uncorrected for skin contact and blood volume changes that obscure the heartbeat. FIG. **20**B shows the same data, corrected for probe movement, which reduces probe movement noise but does not correct for blood volume changes with body movement.

[0065] FIG. **21** shows raw data at six wavebands collected from a human subject during an exercise protocol.

DEFINITIONS

[0066] For the purposes of this invention, the following definitions are provided:

[0067] Ambient Light:

[0068] Light present in the environment. Ambient light is often broadband, that is available over a wide range of wavelengths to perform a detection or analysis, for example by solution of multiple simultaneous spectroscopic equations using a set of optical filters over a sensor. Sunlight is one type of ambient light. It appears white or off-white to the eye, and is also broadband (as defined below). Room light is another type of ambient light, and is of often broadband as well.

[0069] Loose-Fit:

[0070] A device or sensor that, during movement, allows for a sensor to lift away from the body, without contact, but still allowing the sensor to continue monitoring. In contrast, most heart and respiratory monitors are tight-fit, requiring constant, snug contact with the skin or tissue of the subject being monitored. A tight fit forces light to travel into the skin, rather than reflecting back to the sensor, reduces blood movement in low-pressure venous compartments, and blocks ambient light from reaching the detector.

[0071] Compartment:

[0072] A compartment is a location distinguished by temporal or physiological features that differentiate it from other locations. For example, the skin surface (which reflects and scatters light) can be one compartment. Muscle and tissue is another. The arterial bloodstream is a third example, and it differs in many respects (pressure, oxygenation, compliance) from the venous bloodstream, a fourth example of a compartment. Any region that can be differentiated based on such temporal or physiological characteristics can be a compartment for separation, localization, and computational analysis.

[0073] Occupancy:

[0074] The presence, absence, or count of the living bodies in an area. An occupancy sensor could turn on a light if one or more human heartbeats are detected in a room (as opposed to or in addition to using motion to turn on the light), or an occupancy counter could turn up the air conditioning if 5 or more people's heartbeats are seen in a room. Processing spectral analysis of heartbeats using an image sensor with repeating groups of spectral sensors used to create "spectral pixel" groups, repeated as N×N over an image sensor would

allow heartbeats to be spatially detected, temporally auto-correlated to establish identity, and counted.

[0075] Hydration Status:

[0076] The overall water and fluid balance of an individual. In the simplest view, hydration reflects whether an individual has sufficient, insufficient, or excess body water. More complex analysis can look at which body compartments have water (such as intravascular fluids, extracellular fluids such as tissue edema, intracellular fluids).

[0077] Reduced-Power:

[0078] Power consumption lowered as compared to similar sensors through the use of ambient light as a light source for some or all of sensor detection. Reduced power can be a relative term. For example, a sensor and LED system that does not require a lit broadband LED lamp at all times will use less power than an otherwise comparable design that always requires a lit broadband LED, allowing the ambient light system to operate on average at a lower power than a white LED dependent system. A reduction in power consumption by 20% would be considered reduced power.

[0079] Respiratory Rate:

[0080] The rate at which breathing occurs. Breaths may be effective, ineffective (such as during obstruction), or even absent (such as in coma, or during certain types of sleep apnea). There are standard measures known to those skilled in the art, include breath volumes (tidal volumes), and the amount of air moved each minute (minute volume).

[0081] Content-Blind:

[0082] A gesture or event sensing approach that is dependent on a physical act or movement, but is insensitive to state, type, identity, or condition of the gesturer (subject) or object. For example, pressing a key on a keyboard is content-blind, as it does not matter if it is a pencil, a dead cat's paw, a monkey with a banana, or a user's finger that places physical pressure upon the keys or icon. In the view of typical smart phone keyboard, only the physical pressure of the object pressing the key (or for gesture sensitive devices, the movement of the touching object) is important, not the identity of the object doing the actuating.

[0083] Content-Aware:

[0084] In contrast to content-blind sensing, a sensing approach or system in which the sensor is able to intelligently detect and extract certain features about the person or object triggering the sensing event. For example, to analyze and detect that a hemoglobin-containing living hand or a chlorophyll-containing leaf appears in a photographic image are content-aware determinations. Content-awareness allows, for example, a proximity sensor to recognize that an object near a sensor is a living hand or finger, rather than a sleeve or a book, for specific gesture recognition with reduced error. This is not merely a pressure based or touch based system, such as a grip pressure sensor, but an actual spectral analysis to determine the type or state of the target, such as detection of hemoglobin, or changes in the hemoglobin concentration or volume in the bloodstream. Similarly, the color correction of a photograph can be improved if an image sensor is able to determine that a certain feature is human skin, or that another feature is sky, based on a spectral analysis of (or in additional to using traditional image processing of) the spectral information obtained by the sensor.

[0085] Bio-Aware:

[0086] A content-awareness that detects features of a living subject, such as the presence of hemoglobin, a heart rate, a body metabolism, a specific body composition, or recognition that an object near a sensor is a hand or finger for body-specific gesture recognition. A camera that color corrects pixels, or counts living objects present, based on the detection of hemoglobin in the one or more pixels, is bio-aware. This again is more than mere physical detection (such as a facial recognition algorithm using the shape of eyes and mouth) that would be fooled by a color photograph. A bio-aware method determines formal content such as chemical composition, not just physical appearance.

[0087] Filter:

[0088] A device that restricts incoming light to of a specific type of light, such as by wavelength range, polarization, or other optical feature.

[0089] Spectral Filter:

[0090] A filter that specifically restricts incoming light based on color or wavelength, usually restricting it to a predetermined set of colors or range or wavelengths, referred to herein as a waveband. For example, a narrowband interference coating that more or less allows only wavelengths from 550 to 560 nm to pass is a 10 nm bandwidth spectral filter for the waveband from 550 to 560 nm. Typical filters are Gaussian or have nearly vertical square sides, and each presents its own manufacturing advantages and challenges. For example, coating onto photodiodes is more difficult than coating on glass, as glass can survive much higher deposition temperatures without losing shape or function.

[0091] Sample or Target Sample:

[0092] Material illuminated then detected by a sensor for bio-aware spectrally resolved analysis. A target sample may be an object, or can be living tissue.

[0093] Target Indicator:

[0094] An optical characteristic specific to the target being measured.

[0095] Scattering:

[0096] The redirection of light by a target sample. Most biological tissues scatter light, which is typically why we can see or detect them from light that scatters back from living tissues onto our retinae.

[0097] Light:

[0098] Electromagnetic radiation from ultraviolet to infrared, namely with wavelengths between 10 nm and 100 microns, but especially those wavelengths between 200 nm and 2 microns, and more particularly those wavelengths between 400 and 1900 nm where chemical bands appear that allow unique identification.

[0099] Broadband Light:

[0100] Light produced over a spectrally continuous and wide range of wavelengths (called the spectral width, spectral range, or bandwidth) sufficient to perform a detection or analysis, for example by solution of multiple simultaneous spectroscopic equations using a set of optical filters over a sensor. The broadband light could be ambient (such as from sunlight or room light), or it could be produced by sources such as a white LED integrated into the sensor. Spectral width is typically measured at some fraction of the peak intensity over the region of interest, such as full width half max (FWHM), full width quarter max (FWQM), or even full-width tenth max. For some purposes, a broadband range of at least 100 nm can at times be sufficient, while an exemplary sensor embodiment uses a white LED that produces light over 300 nm or more from 440 to 740 nm, with additional light is produced in a second broadband range of 880-1020 nm to provide additional analysis power, may be used. Ambient

sunlight is broadband and covers a full UV, visible, and IR range from below 400 nm to above 2 microns.

[0101] Narrowband:

[0102] The opposite of broadband is narrowband, and less than 50-100 nm in most cases. As a comparison, monochrome LEDs (non-laser, non-superluminescent) are often narrowband, with 20-70 nm widths, while narrowband filters used in the embodiments and examples herein can ideally be as narrow as 5 nm to 15 nm wide, with some more wide or more narrow.

[0103] Light Source:

[0104] A source of illuminating photons. A light source can be external, such as sunlight.

[0105] LED:

[0106] A light emitting diode.

[0107] White LED:

[0108] A visible wavelength LED that appears white to the eye. For the purposes of this embodiment, the white LED is often a broadband white LED comprised of a blue LED and a broad-emitting blue-absorbing phosphor that emits over a wide range of visible wavelengths. Other phosphors can be substituted, including Lumigen or quantum dots.

[0109] Wearable:

[0110] A sensor or device that can be worn on, in, or near the body, such as smart glasses, smart jewelry, or clothing with embedded sensors. The wearable can be an electronic device, like an earphone, an ocular implant or contact lens, a mouthpiece, tooth cover, prosthesis, or a monitoring band.

[0111] Motion:

[0112] Movement, such as running during exercises.

[0113] Non-Contact:

[0114] A measurement in which the detector and/or the illuminator is not in contact with the tissue. This can be a short distance (such as a 2-10 mm spacing under a loose wristband), a medium distance (such as a security and movement detector on the ceiling of an office room, or an occupancy sensor or counter used to control illumination power), or a quite long distance (such as a glasses based sensor that overlays the heart and respiratory rate on people in your visual field even if both of you are in motion).

[0115] Hemoglobin (or Heme):

[0116] A pigmented molecule that carries oxygen in the blood. It is relevant to this invention that hemoglobin comes in many forms. In humans the primary forms are oxyhemoglobin (heme with oxygen) and deoxyhemoglobin (heme without oxygen). The reddish color of arterial blood comes from oxyhemoglobin being the main pigment (arterial hemoglobin is often over 96% oxyhemoglobin and under 4% deoxyhemoglobin), while the bluish color of venous blood is from the presence of large amounts of deoxyhemoglobin (venous hemoglobin is often around 30% deoxyhemoglobin with only 70% oxyhemoglobin).

[0117] Software:

[0118] Software coded instructions for performing the method and algorithms taught herein are code stored on a non-transitory physical media, and are intended to direct a processor with memory, dedicated application-specific physical integrated circuit (ASIC), phone, fitness product, or other physical sensor systems to collect, analyze, and produce results from data collected from the sensors.

[0119] Measurement:

[0120] A non-transient value determined over a period, or at one instant of time. A measurement is a stable form of information that can be stored in machine-readable hardware, such as a memory location, or can be used in mathematical equations or analysis.

DETAILED DESCRIPTION

[0121] One embodiment of the device will now be described. This device has been built, and tested in the laboratory and on living subjects.

[0122] In the device source shown in FIG. **1**, smart phone **101** has illuminator **103** and image camera detector **141**. Illuminator **103**, detector **141**, and the processing, control circuitry, memory, and software together form sensor **102**.

[0123] Illuminator **103** is a white LED. Broadband white light is emitted forward, in a beam as shown by light path vectors **114**, with some light reaching (and optically coupled to) target site **125**. Of note, target **125** is shown for illustrative purposes as a human subject, and is neither a part of the apparatus or system, nor is the human body or human subject claimed as patented material.

[0124] A portion of the light reaching target **125** is scattered and reflected, and returns as returning scattered and reflected light **128** into the smartphone camera image detector **141**. Optionally, detector **141** could be a point detector, a linear array, or even one or more discrete detectors, provided that data representing filtered returning scattered light from the target sample is sensed and measured.

[0125] In this embodiment, detector **141** has added spectral filter **155**. This filter allows only light of a certain color range onto certain pixel elements of detector **141**. In this case, filter **155** may cover only a small region of the image sensor, so as not to interfere with image collection for other purposes, such as photographs. Filter **155** in this example has 7 narrowband filter ranges, each 5 nm FWHM wide, with center wavelengths at or near 525, 540, 555, 570, 585, 600, and 630 nm. Additional ranges may include filters with center wavelengths at or near 900, 920, 940, 960, and 980 nm for fat and water detection, and for these wavelengths in phones with white LED illumination, the 900-980 nm illumination must come from an infrared (IR) source in the phone's illumination or from ambient or other illumination sources). Sensor **102** measures less than 3 mm in width. Another range could be predetermined filters with center wavelengths at or near 445, 465, and 485 for the detection of bilirubin, the pigment of jaundice. Other filter sets could be selected for the detection of other compounds such as grain alcohol, sugar, abnormal hemoglobins, hematin (found in cells infected with malaria), and other biologically relevant pigmented molecules. Filter **155** is attached to detector **141** using optical epoxy.

[0126] The non-contact measurement can be enhanced using polarization filters, integrated into the emitter and at **90**-degrees (cross-polarized) on the detector. This is because light that reflects off of the skin retains polarization, and can be blocked using a correctly positioned polarizer on the detector (in this case cross-polarized, but it may be a different angle in other situations). In contrast, light entering the tissue is depolarized during multiple scattering, and thus travels in greater percentages through the cross-polarizer on return, thus enhancing the light. In studies, we found that the apparent hemoglobin (a measure of travel through tissue) was up to 2-fold higher when crossed-polarizers were used. These are shown in FIG. **1** as a polarizer layer included as part of the construction of filter **155**, and optional polarizer **181** over illuminator **103**.

[0127] Next, some or all of the data from image detector **141**, including the filtered pixels, is read and processed by embedded microcontroller processor **187** (such as those typically present to operate cell phones, and shown dashed as it is located internally as part of the cell phone main circuitry) based on machine-readable code **193** saved on physical media, such as ROM or flash disk memory **191**, connected over electrical connection **195**.

[0128] The machine readable code may optionally be system software saved as a machine-readable code embedded within a non-transitory physical memory ROM, or it could be an "app" (a downloadable code available for installation and/or purchase and then stored within a non-transitory physical memory), or it could be an "API" (an installed driver for a specific sensor, such as would be provided by a manufacturer with a given physical sensor set and using instructions stored on non-transitory computer readable media).

[0129] The precise design of software **172** will depend on the smartphone, watch, earbud, anklet, camera, or bracelet processor, but its function is to process the image and provide raw or processed results to the device or system For example, one result would be the photon counts for each of the filtered region, with each filter region covering multiple image pixels. Another result could be a processed result, in which least-squares fitting is performed against a spectral standard in order to determine the presence of hemoglobin in the image. Another result could be that the measurement is processed over time in order to produce a heart rate estimate. Each of these falls within the spirit of the invention if the returning light is processed for type, state, identify, or gesture, and if the broadband white LED source is used for illumination.

[0130] Spectral filter **155** of this preferred embodiment is now briefly described, as shown in FIG. **2**. Here, filter **155** is shown as all of FIG. **2**A and composed of 7 optical fibers **205**A through **205**G (one or more wavelengths described in Example 1 are omitted for clarity). The number of fibers can vary, even down to 1 but more typically 3 to 12, depending on application. Each of the fibers has a spectral filter coated onto the top end of each fiber, and the filter differs for each fiber **205**A through **205**G. In this example, the fibers are arranged in a circle of 6 outer fibers, with one central fiber. Alternatively, the fibers can be in various layouts, including different shaped patterns (square, linear row, star). In the construction of this custom filter, the fibers are first provided a filter coating, with each wavelength range run in a separate deposition chamber using pre-cut pre-polished (or cut) fibers, with thousands or more in each deposition chamber run. Then, one fiber of each wavelength is taken, prepared with epoxy on the side of the fiber, and placed into glass tube **211**. Alternatively, tube **211** could be plastic, epoxy, resin, metal, or other material, provided it allows alignment and securing of the fibers. Once the black epoxy, shown as black epoxy **217**, hardens, then distal end **225** can be polished.

[0131] A photograph of an actual 7-fiber system we constructed is shown in FIG. **2**B, where all fibers (except fiber **205**E) are illuminated. The image and localization improves with better polishing, spectral filter deposition, and other improvements to the fiber tip. This tip as shown in FIG. **2**B can then be glued directly to detector **141** as shown in FIG. **1** as filter **155** on detector **141**. The fibers are then attached (in this case, clear epoxy optical glue) to the face of the CCD for direct transfer of the transmitted photos to the image sensor detector.

[0132] Alternative constructions are optionally possible. For example, there may be more or fewer than 7 filter ranges, depending upon the intended application. Next, there may be more than 1 fiber for each wavelength range. For example, there may be 10 of each fiber, for a total of 700 fibers in the set. Then, after placement on the CCD, a calibration may need to be performed to assign each image sensor region to a pixel spectral range, allowing averaging and integration at several locations for each range.

[0133] Another alternative format for filter **155** as used in sensor **102** is shown as FIG. **2**C. Here, the filter is comprised of a number of small filters assembled on one or more silicon detectors **141**, shown as filters **235**A through **235**H, which are placed over the surface of detector(s) **141**. Amplification and processing of the signals occurs in integrating amplifiers, and microcontroller processors, and instructions stored in non-transient machine-readable physical memory **244**.

[0134] A photograph of such a device as constructed and tested is shown in FIG. **2**D, where custom optical filters **235**A-D and **235**F-H (Omega Optical, Brattleboro, Vt.) with collimating lenses can be seen on top of silicon photodiodes or phototransistors. Here elements are added above the silicon detectors to complete sensor chip **102**, such as a collimating spacers, polarizers, and focusing lenses can be added, such as to reduce the angular bleed through of light into the spectral filters. The darker-appearing detector has only transparent region **235**E in FIG. **2**D, and no collimating lens, allowing unfocused and spectrally unfiltered white light to reach the detector).

[0135] A schematic of a sensor chip is shown in FIG. **2**E. Here, sensor board **250** has microcontroller processor **253** (which can be an off-board controller) using LED power control **255** to power white LED **257** configured in flash mode. Light travels without tissue contact along light path **263** to a body part. As in FIG. **1**, the human body and tissue are shown only to provide an understanding of the operation of the device, and the human body is not considered to be a claimed part of the present invention. Light scatters through the tissue along light path **265**, and then leaves the tissue along backscattered and remitted light path **269**, re-encountering sensor chip **250**, and entering filter and photosensor detector array **272**.

[0136] As described, the spectral filters can be separate elements, one filter element tuned by angle of entry across a range, or filters deposited directly on the detector substrate. In this case, interference filters were on separate glass substrates (custom 3×3 mm filters, Omega Optical, Brattleboro, Vt.) ranging from 5 to 40 nm FWHM, and were glued on each photodiode detector using optical quality UV set glue. A polarizer and lens were additionally added to the stack above each filter. The detector may be CMOS, a photodiode, a phototransistor, or any number of suitable optical detectors known in the art. In this example, the detectors are 8 photodiodes (Vishay temd7000 or larger). Alternatively, spectral filters could be replaced by a spectral grating that filters the light by spatially separating the wavelength into discrete wavebands over each physical region of light striking a detector.

[0137] Detector array **272** creates an output measureable amplified and digitized by amplifier and A-to-D converter **274**. In this case, the detector outputs are captured and integrated by low noise CMOS or BiFET amplifiers (analog devices AD823A), and translated to 16-bit digital sample/hold A-to-D converter (Linear LTC1867L). High gain chan-

nels reach 66% saturation at 16 uW/cm^2. The measurement can be improved by use of MOSFET amplifiers, and also by using higher-gain phototransistors, or even avalanche photodiodes (though the required avalanche bias may increase the complexity of the chip and the cost of the sensor). Background estimation can be done by flashing the light at brief intervals. Each measurement filter channel is low pass filtered in two passive stages using a 1.2 ms time constant to control noise, and the light source itself is flashed on for 2 ms before a reading is taken. The system using less than 1 mm^2 of photodiode at each wavelength operates with 8-bit effective signal. By using a full 7.6 mm^2 from a 3×3 mm detector photodiode, 11 effective data bits can be obtained in this manner. For heart rate hemoglobin pulse signals, 8-14 bits is recommended. As shown in shown in FIG. **2**E, signals leave board **250** and are transmitted over link **279** to a bracelet, band, watch, earbud, phone, or other device. Link **279** can be an I2C wire, or even a Bluetooth connection (such as Bluetooth Low Energy, or Bluetooth LE). Sensor **102** may encompass both board **250** as well as device **280**, either as a standalone sensor or as an embedded system within another system, device, wearable, article of clothing, camera, sensor, or other device. Here, device **280** includes machine-readable non-transient machine code stored in stable, readable ROM **288**, and executed in this case as app layer **283** running on processor **286**. Display **292** may provide results, feedback, warnings, or upload confirmations to a user. It may even display messages from a concerned physician who is responding to the data collected by sensor **102**.

[0138] Alternative formats are also possible for the broadband light source instead of using a single white LED.

[0139] Ambient sunlight is broadband and covers a full UV, visible, and IR range from below 400 nm to above 2 microns, while room light LEDs are increasingly found to be white broadband LEDs. Alternative formats are also possible for an optional additional light source that may be needed to produce broadband light when the ambient light is dim.

[0140] Another example is a multiple LED source, shown in FIG. **3**A. Such a combined LED may be required when measuring, for example, fat and water using the spectral peaks in the 700-1000 nm range, a region not supplied by most conventional white LEDs found in ambient room light or in the white LEDs found in some cell phones and other mobile devices. Here, frame **312** with bottom **316** and opening **318** holds multiple LEDs **332**A to **332**N. These multiple LEDs, which can include broadband LEDs such as a white LED, are inserted into frame **312**. Light from the multiple LEDs is focused or concentrated out exit opening **318**, to provide broadband light.

[0141] When manufactured, the light source can be significantly more compact, as shown in the photograph in FIG. **3**B. Here, multiple LEDs **332**A through **332**N are surface mount LEDs on PC board **335**.

[0142] Light output from this multi-element light source is plotted in FIG. **4**. Here, light emission is detected from about 700 nm to over 1000 nm, with light usable for over 300 nm of spectral width, from mark **451** to mark **463**, with very little light by mark **425**. Of note, the spectrum plotted shows peaks at peak **432**, peak **434**, peak **437**, and peak **439**, reflecting the peak contribution of certain LEDs used to build the light source. The width of the light output is shown as spectral width **457**.

[0143] Operation of the device may now be described.

[0144] Smart phone **101** is turned on, and the spectral physiology app is selected by the user and started. For example, in an Android system, the app icon is located and touched, launching the app.

[0145] The app turns on phone white LED **103** and begins to collect data from camera detector **141**. Data from detector **141** is accessed using software, in this case written in android language and compiled using the Android software development kit (SDK), available online (for example, at http://developer.android.com/sdk/index.html). Image data from detector **141** is available as RGB data (or as luminance and color, convertible to RGB using known equations). However, under spectral filter **155** the image from the lens is replaced by data from the fiber ends. An example of such data is shown in the image in FIG. **1**, in this case collected using a USB plug in camera for a PC computer, dissembled and modified to have filter **155** attached and glued to the surface. The app software has already been calibrated to know which image pixels correspond to which filter, such as fiber center region **234**A in FIG. **2**B, and to ignore the overlap areas between fibers where two or more fibers overlap, such as fiber overlap region **234**B in FIG. **2**B. With many pixels of a detector covered by this filter, one may average the pixels to add statistical strength. What is produced by this combination is a table of the intensity at each of these wavelengths, which can then be analyzed in various ways.

[0146] This data may be collected on a spot basis for measurements without real-time change (such as water/fat composition), intermittently for values that change over minutes (such as cardiac performance), and nearly continuously (such as every 50 ms) for values such as heart rate, for which a continued change is key to extracting the value. These determinations are shown in more detail in the illustrative examples that follow.

EXAMPLES

[0147] The breadth of uses of the present invention is best understood by examples, provided below. These examples are by no means intended to be inclusive of all uses and applications of the apparatus, merely to serve as case studies by which a person, skilled in the art, can better appreciate the methods of utilizing, and the scope of, such a device.

Example 1

Non-Contact Heart Rate Determination

[0148] In this example, illuminator **103** is a white LED embedded into a Samsung Galaxy S3 smartphone. Software app **172** is a custom software loaded into a machine-readable physical memory (4 Gb microSD card, San Disk) placed into the external SD card slot of the Galaxy phone, and installed using the Android operating system (Android 4.4, Google) on the phone. The app is launched using the Android touch interface. Multiple filters allowed multiple bands wavelength bands to be collected.

[0149] Upon launch, Software app **172** turns on illuminator **103**, as well as displays a camera image from detector **141**, which shows a hand placed into the image sensor view, but not necessarily in contact with the sensor. A pixel region corresponding to sensor intensity averaged over 100 pixels for each of these spectral ranges every 300 milliseconds is captured.

[0150] After capturing a spectral channel, the intensity is processed for change over time (a differential plot of intensity changes with respect to time). Here, the value is plotted versus time. The data are shown in FIG. **5**A.

[0151] In FIG. **5**, a time-varying output can be seen. In this case, the value of the output is determined as the normalized measurement from the 570 nm channel, minus a baseline change correction from a base-correction average of the measurement in the 460 and 630 nm channels. From this heart rate can be calculated simply by counting the peaks, using any of a number of methods familiar to those skilled in the art. One exemplary approach is to determine the beat-to-beat interval (i.e., the time between peaks). This allows for beats that are dropped to be detected as double-wide intervals which can be rejected, producing a more stable measurement in response to movement noise.

[0152] Alternatively, raw data, or interim determinations such as intensity changes over time, may optionally be displayed. Also, simply the changes in intensity at 570 nm (or other channels) may be plotted, as in a stable lighting environment the major change over intervals of seconds is the absorbance change caused by changes in hemoglobin.

[0153] For processing, a first differential (with respect to time) is determined, producing the varying measurement shown at plot **540** in FIG. **5**A. Here, varying intensity **546** has peaks and troughs, which correspond to changes in hemoglobin volume with the pulsing of the heart. Peaks can be seen at **551**, **553**, **555**, and **557**. Each of these corresponds to one heartbeat. By determining a heart rate using the beat-to-beat intervals, and discarding the intervals with dropouts, a heart rate is determined; in this case, a heart rate of 72 beats/minute is measured and displayed.

[0154] Next, we constructed a research probe that allowed the sensor and broadband light source, of the types shown in FIG. **1** and constructed in accordance with the present invention, to be incorporated into a loose wristband system, with data collected at a multiple wavebands. How the data are processed to correct for physiology and motion are described in detail in later examples (for example, in Example 18 to Example 20).

[0155] Rather than use other indirect measures, such as other fitness monitors, we have compared the performance of this wristband to a chest electrode EKG, to test accuracy. Data were recorded from a human volunteer during an exercise protocol, as described in the previous example. This subject also wore an accelerometer, a pulse oximeter, and several other instruments that monitored multiple functions during the study.

[0156] The heart rate signal, as determined in accordance with the present invention in the previous example, in this case using 8 waveband multispectral data, is shown as plot line **582** in graph **586** of FIG. **5**B. Also recorded at the same time, and plotted in FIG. **5**B are the multiple, repetitive, narrow spikes of the QRS complex from a gold-standard chest lead EKG, shown as plot marks **588**. The EKG records the electrical pulses from the heart with millisecond accuracy (when measured at 250 Hz with interpolation).

[0157] Comparing the signals visually at first, it can be seen by eye that there is a peak in the calculated heart rate signal with nearly every electrical signal, and very few such peaks visible where there is no EKG signal. This validates that the arterial signal has been extracted accurately, and that the timing of the signals is not invalidated by the EKG.

[0158] Instead of a visual assessment, another method of assessing the accuracy of these measures is to determine the interval between heartbeats, in milliseconds between beats or in effective heart rate at a given interval (e.g., an interval of 500 milliseconds corresponds to 120 beats/min), and compare these two measures. This beat-to-beat interval can be compared on a beat-to-beat basis, or averaged. In this following example, interval data were plotted as a running boxcar average over a moving 5-second window.

[0159] Several points are of note.

[0160] First, measurement of the heart rate occurred during hard exercise, and would have been noisy or unreadable if using just one wavelength. In order to perform this calculation, multiple wavelengths were used to correct for movement artifact, and pulsations that resulted from movement of blood in the body.

[0161] Second, from this heartbeat data, a heart rate can be calculated. A single point sensor can also be used (zero-D), or a linear array can be used (1-D), instead of or in addition to the image sensor (2-D). An image sensor would allow this measurement to be seen at many pixels, allowing a heart rate to be determined across an image.

[0162] Next, it is not required that the sensor have contact with the subject. The heart rate sensor could be a white LED mounted in an exercise machine, with an image sensor in the display panel of the exercise machine measuring the exercising subject without contact.

[0163] Next, the sensor is not limited to measuring the heart rate of a wearer or user. The image could use the same algorithms to extract heart rate from a room full of observers, such as during a poker game or a business meeting, or at an airport checkpoint.

[0164] Also, as cardio-workout is defined in terms of minutes of elevate heart rate (either above baseline, or as a percentage of maximum ideal heart rate), one could auto-calculate the minutes of cardio workout in any day, automatically, so that the user does not have to see heart rate graphs or tables, merely seeing just the minutes of ideal cardio-workout per day for example.

[0165] Also, from the above example, it is clear that multiple analyses can be performed on different regions of the sensor, allowing multiple people to have measurements such as heart rate measured for each person either simultaneously, or by selection. The approach is not limited to one target subject, nor to the wearer of the device. The determination could be from a glasses-mounted device that displays the heart rate of those around the wearer, and displays these results for the wearer to view.

[0166] Next, multiple image sensors could allow such data to be collected from groups of subjects in more than one location, such as from different rooms or different checkout aisles.

[0167] Next, note that there is some baseline variation. The size of the pulse signals varies with respiration. Because of this, a respiratory rate signal can be derived, and this can be used to estimate respiratory rate from optical data from wrist, ankle, or face, using measurements obtained even at a distance.

[0168] Next, such measurements are not limited just to heart rate. Screening for medical diseases (such as anemia, tachycardia, heart rhythm irregularities, jaundice, malaria, heart failure, diabetes, jaundice), chemical levels (alcohol, high cholesterol), or even fitness can be screened.

[0169] Next, because the measures can be broadband, the background light, which varies according to optical contact or coupling of the light to the subject, can easily be subtracted. For example, a baseline may vary widely as a subject runs and moves with a loose fitting heart rate sensor. However, once the baseline movement is corrected (all wavelengths will change, unlike the heart rate measurement which involves only some of the wavelength spectral channels), the background corrected values will more clearly show the hemoglobin variation that represent the changes with heart beats (e.g., heart rate). This allows a non-contact measurement that is resistant to movement, motion, changes in position, changes in background light (such as running in and out of the shadows of trees), all because the broadband values are oversampled, with excess data that allow for background light correction.

[0170] Last, because this approach involves broadband light, even background lighting can be used to extract the measures, such as room light in a meeting, or sunlight on athletes working outdoors. This can allow elimination of the white LED.

Example 2

Content Aware Detection

[0171] As an example of content awareness, one use of the detection of these features is the ability to detect tissue.

[0172] Conventional proximity detection involves either an intensity measure that changes as tissue moves closer or farther away, or uses a distance monitoring method to detect the distance from the sensor to the nearest object. Both of these approaches have problems. Both of these methods would view a piece of paper moving closer as the same as a face moving closer. That is, they are neither content-aware nor bio-aware.

[0173] In a study performed with human volunteers, a hand was moved over a sensor constructed in accordance with the present invention. The presence of hemoglobin at a tissue saturation level expected in human subjects was used as a measure of the presence of living tissue, and the observed intensity of the signal was plotted as a proximity signal. Also calculated was a pure intensity only signal, which is the standard proximity signal.

[0174] Data are plotted in FIG. **6**A-B.

[0175] In a first study, data are shown from a hand passing over the sensor, as shown in FIG. **6**A. Here, standard proximity signal is shown as a dashed line, starting at a low value before viewing the skin is seen at point **613**, then rising to a maximum when the hand is seen at time point **615**, then falling again at time point **618** as the hand moves past the sensor. This rise and fall would be consistent with a detection of the hand by a standard proximity sensor. A similar pattern is seen by the bio-aware proximity sensor, starting at point **623**, rising to a maximum at **625**, and falling again at point **628**. In this case, both the standard proximity sensor and the bio-aware proximity sensor return the same result.

[0176] Next, the study is repeated, only this time with a piece of inanimate cloth over the wrist passing over the sensor, as shown in FIG. **6**B. Here, standard proximity signal is again shown as a dashed line, starting at a low value before viewing the sleeve is seen at point **633**, then rising to a maximum when the sleeve is seen at time point **635**, then falling again at time point **638** as the sleeve moves past the sensor. This rise and fall would be consistent with a detection of the sleeve by a standard proximity sensor. In this case, with the skin covered, a different pattern is seen by the bio-aware proximity sensor, starting at point **643**, failing to rise to a maximum at **645**, and remaining low at point **648**. In this case, the standard proximity sensor and the bio-aware proximity sensor return different results, because the bio-aware sensor does not detect any living tissue within the field of view of the sensor.

[0177] This bio-aware sensing can have many purposes.

[0178] For example, a security device could trigger an alarm not just when motion is detected, but when human hemoglobin or a human pulse is detected. This security device could be made to distinguish human hemoglobin from other animal hemoglobin, such that a dog in the security camera view would not trigger an alarm, even if moving. Because the determination can be performed in a non-contact mode at a distance, the technique could be integrated into video cameras, ceiling sensors, lampposts, and the like.

[0179] Similarly, the bio-aware sensor could be used to control illumination. In this case, it is not security that is the issue, but energy efficiency. The lights in a room controlled by a motion sensor will turn on when a subject enters, but turn off when the same subject sits still at a computer monitor. A bio-aware device would turn off the lights only when the living human leaves a room, and there is no remaining human hemoglobin or human pulse in the room. Similarly, the lights would not turn on when the family dog enters the room, as the detection would be keyed to human physiological features, while non-human hemoglobin is often spectrally quite distinct from human hemoglobin.

[0180] Next, the device could distinguish between real and sham tissue, such as for unlocking security sensors that are image based (such as fingerprint sensors that can be fooled by photocopies of fingerprints).

[0181] Next, the device could be used to turn on or off phones when the screen is placed against a face by detection of the human tissue.

[0182] Next the sensor could be used to detect where a laptop or tablet is being held, to distinguish human touch from the pressure of a pocket or table.

[0183] Last, because different people have differing body composition (fat/water/melanin), different skin thicknesses, different levels of tanning, are of different races, age, gender, and ethnicity, this content awareness could provide some identification features. For example, even without a fingerprint being entered (for instance, if a cell phone is unlocked but is grabbed or picked up by an unauthorized user), then the normal composition of the user in terms of the above characteristics could be used to identify the user, and lock out an unauthorized user who is holding the phone. Similarly, markers (such as dyes, tattoos, unique mixtures of quantum dots) and the like could be used to make very specific optical markers that are nearly impossible to forge, due to the large number of admixtures of different wavelengths of quantum dots (perhaps hundreds could be distinguished) as well as each type having a relative ratiometric concentration, sensitive to one part in 2 raised to the 16^{th} power, or more. As each agent could be in various concentrations, this alone would yield 2 to the 20^{th} mixtures, even without a spatial tattoo patterning. Such implanted dyes could be encapsulated to be stable, providing non-radiowave, optical identification difficult to reproduce or transfer. Combined with a live dead detection, a high level of security could be achieved.

Example 3

Heart Performance from a Bracelet Monitoring

[0184] In this example, a bracelet was constructed using a white LED light and an optical fiber. The optical fiber allowed for ease of construction, in that a silicon sensor did not need to be incorporated into the small wristband. Rather, the light was transferred from the optical fiber to a commercial spectrally resolved linear sensor and measurement system (T-Stat 303, Spectros Corp, Portola Valley, Calif.) operating in a data-recording mode. This device is a commercial system incorporating a spectrophotometer (Ocean Optics SD-2000+, Dunedin, Fla., USA) to measure light entering the system. Data is recorded on an internal disk, then exported to a USB solid-state drive for storage and analysis, in this case in excel on a laptop computer.

[0185] A fit subject was exercised on an elliptical trainer. The power of the workout (joules/hour), the subject's heart rate, respiratory rate, work power, and pulse oximeter reading were recorded using other monitors, including a video recording for synchronization of the various data during analysis. Selected resulting data are plotted in FIG. **7**.

[0186] In FIG. **7**, a measure of cardiac performance is calculated, as the reciprocal of the arterio-venous difference, defined as [1/(SaO2%−SvO2%)]. For this, the SaO2% was estimated using a pulse oximeter, SvO2% was estimated from tissue oximetry of the wrist from data collected from the bracelet using known SvO2% determination algorithms from spectral data, and the data were normalized to 1.00 at the start of the study. The SvO2% measurement was performed using spectral fitting to data from the wristband using tissue oximetry. In practice, a wristband would use the same approach as shown in Example 1, using a white LED, a silicon imager and a spectral filter, and a computational spectral analysis to the spectral data using least squares fit of the spectral data to separate data into component compounds or compound types, such as various forms of hemoglobin, using oxygenated and deoxygenated hemoglobin standards.

[0187] Data are shown in FIG. **7**. Here, cardiac performance is 1.00 at the start of the study, at point **713**. As the subject begins to exercise, performance rises to peak at point **718**, then returns to near baseline after recovery to point **721**. Also seen are 60-second rest periods at time points **733**, **735**, and **737**. Even during the short rest period, the recovery of heart function is seen. Note also that during this exercise recording, a pulse oximeter readout (medically called SpO2%) remained at 96-98%, and also that the heart rate measured did not recover substantially at all during the rest periods (not shown). There were large dropouts in which the pulse oximeter further was unable to read at all due to motion artifact.

[0188] Last, taking the power of the exercise in joules/hour (as measured from the elliptical trainer, which is an estimated workload in this case as this trainer was a commercial exercise device not a physiology lab device, though we expect the power estimates to roughly track a physiology device) and correlating with the cardiac performance on a scatter plot shows that among heart rate, pulse oximeter, and cardiac performance measures, only cardiac performance correlates well with workload (r^2>0.82).

[0189] There are several points to note here

[0190] First, this data was collected with a fiber-based system for ease of laboratory analysis. Use of a mobile system with an LED and a sensor would be one approach to measure these values on mobile athletes. The use of a tethered fiber-optic wrist probe was for proof of feasibility.

[0191] Next, cardiac performance could be one of the first performance based devices available to athletes that measures cardiac performance using a simple, optical, non-contact, wrist-based monitor.

[0192] The form of a monitoring device includes non-contract pendants, cameras, phones, wristbands, and other wearables. The sensors could be incorporated into clothing such as gloves, spandex suits, caps, bracelets, pendants, and the like.

Example 4

Body Composition on a Dieter

[0193] Hemoglobin is one of the most intense and visible pigments in the body, however there are many other pigments that can be measured by this method.

[0194] Fats and water are key body constituents, and have spectral features. Fats exhibit a peak at 920 nm (and elsewhere, including near 760 nm), while water has a peak at 960 nm (and elsewhere, include second differential peaks about 820 nm, large absorbance peaks between 1 and 2 microns, and a broad absorbance peak more or less between 2 and 10 microns).

[0195] We constructed a device that measures in the infrared by modifying a commercial spectral monitor (T-Stat 303, described earlier) to measure on the body. This device has a broadband infrared LED instead of a broadband white LED. As noted above, certain ambient light such as from sunlight, can be used to collect the same raw data instead of light from broadband LED, which would be processed in the same manner as shown in this example. The broadband infrared LED was designed and constructed for the purpose of having wavelengths above the typical white LED visible range, as shown in FIGS. **3**A and B. In this case, light was produced from 650 nm to 980 nm, but any broadband infrared source could be used, including (as discussed under ambient light) sunlight or room light from incandescent bulbs. The spectral peaks were identified using the same fitting methods one would use to fit hemoglobin, such as differential spectroscopy to remove background signal and emphasize the peaks. The concentration of the fat and water was set to 100% by measuring on phantoms containing pure water or fat.

[0196] The table below shows determinations from this system, which measuring on a hand, wrist, breast, and head, as shown in
Table 1, below:

TABLE 1

Tissue/Material	Fat	Water
Finger	12%	65%
Breast	45%	22%
Bicep	15%	61%
Abdomen	33%	42%
Ankle	18%	55%

Components of living tissue include fat and water.
Other substances, such as volume of bone, collagen, and pigments such as melanin and heme, therefore the values do not sum to 100%.
Multiple measures around the body could allow for body composition analysis.

[0197] This detection of composition is also important, as fats, water, and even proteins in the bloodstream can be measured optically, allowing an estimate of calories taken in by ingestion. Together with calorie expenditure monitoring,

taught below in Example 12 and Example 13, this can be used to estimate calorie balance, such as when sufficient or insufficient calories have been ingested in a day (calorie balance), or using the water signal, whether sufficient or insufficient water has been ingested in a day (such as hydration status and water balance).

Example 5

Fat and Water Detection

[0198] Security systems require an identifier in order to detect the presence or identity of a person. Sometimes this identifier is a password or ID chip, while at other times it is a biometric measure (fingerprint, retinal blood vessel pattern). However, some fingerprint detectors can be fooled by something as simple as a cyanoacrylate copy of a fingerprint on cellophane tape.

[0199] By performing the analyses of the above examples (detection of heart rate, cardiac performance, fat/water composition), one can easily distinguish real from sham tissue.

[0200] In this example, we perform the measures listed in the above example. Tissue is measured for hemoglobin (heme) content. Normal tissue is 20-120 uM heme, with a saturation between 30%-80% for SvO2%. Further, living tissue is mostly water and fat, with water and fat comprising 50-90% of the volume in sum total. Further, there should be a low fitting error (for this algorithm, the error from unrecognized components should be below 200 though this number will vary by system and algorithm). Once these features are taken into account, the real, live tissue (as opposed to dead meat, colored paper, or inanimate objects) can easily be recognized, as shown in Table 2, below:

TABLE 2

Once the components and features of living tissue are taken into account, the real, live tissue (as opposed to dead meat, colored paper, or inanimate objects) can easily be recognized.

Tissue/ Material	Heme	Svo2%	Has Pulse?	Fat	Water	Fit Error	Live Tissue?
Finger	51 uM	55%	Yes	12%	65%	68	Yes
Breast	20 uM	71%	Yes	34%	22%	91	Yes
Meat	450 uM	0%	No	15%	61%	122	No
Table top	2 uM	n/a	No	0%	0%	45341	No
Red Paper	1 uM	n/a	No	0%	0%	3911	No

The "n/a" value indicates no value is determined when the material is not human tissue with blood.

[0201] Different subsets of this approach can be taken into account, depending on application. For example, a pulse (heart rate) takes a few seconds to detect, while fat and water can be measured in a microseconds. Therefore, a fingerprint sensor that seeks to verify what is alive and not alive, or real and not real, may wish to use the spectrally determined composition in this analysis.

[0202] A few comments on water detection.

[0203] Water has a spectrum with peaks that allow detection of concentration. While many combinations of wavelengths can be used, combinations that detect differentiating features of the water spectrum are possible. For example, water has a broad peak at or near 960 nm (peak **1825** of FIG. **18**) that differentiates water from the absorbance of fat, hemoglobin with or without oxygen, bilirubin (the pigment of jaundice), and other substances.

[0204] One method of detecting water is to look at the difference between the local baseline from 900 to 1000 nm versus the absorbance at the 960 nm peak of water. Analyzing this peak allows determination in Table 2 of the water content. This is translated to a percentage by accounting for the heme and fat components, and normalizing to standards with 100% of each substance in a light scattering medium such as tissue.

[0205] Similarly, fat content can be determined using the 920 nm fat peak (peak **1833** of FIG. **18**). This peak is often accompanied by a peak near the 760 nm peak of deoxyhemoglobin. A similar peak analysis to that used for water allowed detection of the fat content as shown in Table 2, with normalization as described above.

[0206] Hemoglobin can similarly be solved for one or more of its multiple forms. There is a double peak for oxyhemoglobin at or near 542 and 577 nm (peak **1842** and **1844** of FIG. **18**) and a broader single peak for deoxyhemoglobin at **560** nm (peak **1852** of FIG. **18**).

[0207] More detailed extractions, such as matrix solutions to multiple simultaneous linear equations can be used as well, though these require more processing by the processor executing instructions stored in memory. Such approaches work for bilirubin (with a peak near 460 nm), alcohol (with peaks above 1 micron), cholesterol with peaks around 1.7 microns), and other pigmented components in the bloodstream.

Example 6

Incorporation into Systems and Devices

[0208] The sensor as described can be incorporated into a small sensor or device.

[0209] Several devices incorporated into systems are shown in FIG. **8**A through FIG. **8**G.

[0210] A loose fit wristband is shown in FIG. **8**A. Here, loose-fit wristband **814** has sensor **818** integrated into its body. This would allow a fitness band, as well as a monitor for persons with chronic medical disease.

[0211] A medical or fitness wristwatch is shown in FIG. **8**B. Here, wearable watch **821** has sensor **818** integrated into its body or strap. Display **823** shows a user certain useful information, including heart rate **826**. This would also allow for a fitness band, as well as a monitor for persons with chronic medical disease.

[0212] A heart-rate sensing pendant is shown in FIG. **8**C. Here, pendant **832** could hang near the users' body, but not in fixed or permanent contact with the skin, and has sensor **818** integrated into its body. Such sensors could be on two sides, such that one side always senses skin. The proximity sensing and tissue sensing disclosed within could turn on only the side against tissue.

[0213] Wearable glasses with sensor are shown in FIG. **8**D. Here, wearable glasses **844** have sensor **818** integrated into frame or lenses. A display could be added, much as in heads-up displays to show a user useful information, including heart rate, or into a device such as Glass (Google, Mountain View, Calif.). The sensor can look outward as well, and record heart rates in business meetings, road races, and the like. As noted earlier, the face is a strong source of heartbeat pulses, and the decreased motion compared to the legs and arms makes this an excellent source of measurement.

[0214] A remote sensor for ceiling or rooftop mounting is shown in FIG. **8**E. Here, remote sensor **852** has sensor **818** integrated into its body or strap. Additional white LED or infrared illumination is provided by LED array **857**.

[0215] A wearable clothing sensor is shown in FIG. **8**F. Here, shirt or textile **862** has sensor **818** integrated into the textile. Wireless communications could be added to communicate with other devices, such as watch **821** or glasses **844** of FIG. **8**G, or cell phone **101** of FIG. **1**.

[0216] An insertable ear probe, into which a heart rate sensor could be placed, is shown in FIG. **8**G. Here, earbud **875** has sensor **818** integrated into its body or strap. As noted earlier, the ear is a strong measurement source, though this varies from the pinnae to the auricles to the external canal.

[0217] One point of note, different parts of the body have stronger or weaker signals, depending upon what is being sought. For example, the pulsatility at the wrist is often lower than at the fingertips, nail beds, ear lobes, lips, cheek, or forehead, while the ability to measure subcutaneous fat is better over the wrist than in the lips. In contrast, the face has a different venous pulsation with movement than does the wrist. In part, this has to do with the blood flow of the tissue, and the thickness of the skin, but it also is affected by the venous valves present in the arms, but not in the face. Because of this, different sensor configurations, and different algorithms, may be required at different places.

Example 7

Non-Contact Sensor Design

[0218] In this description the terms loose-fit and non-contact are used. Light forced into tissue (such as from an emitter in physical contact with optical elements of the emitter directly into tissue) and detected by an emitter also in direct physical contact with tissue (such as a CCD pressed directly against skin) travels a different average path than light coming from an emitter source, travelling through the air to skin or tissue, and then scattering and reflecting back to an emitter, also at a distance from the tissue. Further, direct pressure to the measured tissue can suppress pulsatility (though minor pressure may suppress the effects of movement more than the pulsatility).

[0219] One way to encourage or ensure the system is non-contact is to place the sensor into a device intended to be kept at a distance, such as cell phone **101** of FIG. **1**, or ceiling security sensor **852** of FIG. **8**E.

[0220] However, such distance is not always possible, especially with wearable devices. In such cases, it may be important at times to force the sensor to remain out of physical contact with the subject, tissue, or object to be examined. In such cases, a design as shown in FIG. **8**A through FIG. **8**C, or the ear buds of FIG. **8**G, may be advantageous.

[0221] Such a hardware method to ensure the sensor is non-contact is shown in FIG. **9**A and FIG. **9**B.

[0222] First, a recessed non-contract sensor with the illumination and detection on the same chip are shown in FIG. **9**A. Here, device **912** has well **927** which holds sensor **933**. Well **927** holds sensor **933** away from the skin, by millimeters to centimeters, making light reflect off of the tissue or objects surface when device **912** is held against the tissue or object.

[0223] Alternatively, sensor **933** can be separated into separate components, such as emitter **944** and detector **946**, with light shield **949** between the two, as shown in FIG. **9**B.

[0224] Note that in these designs, emitter **944** and/or detector **946** may also each be composed of multiple components that are also similarly separated.

Example 8

Measurement of Respiratory Rate

[0225] Breathing leads to increases in pulse size at a time constant determined by the breathing rate, as well as shifts in venous blood proportionate to the depth and effort of respiration.

[0226] During inspiration (breathing in), the pressure in the chest cavity drops, increasing the rate of return of venous blood to the heart. This in turn makes the pulse volume larger, as cardiac output volume for each beat is driven in part by how much blood returns to the heart during filling during the rest cycle. As a result, the pulse size rises and falls with respiration. This produces a volume change in the total arterial blood signal that has frequency of 8 to 30 times a minute (even faster in infants). By analyzing the average beat-to-beat volume changes in the arterial compartment at longer frequencies than typically seen for heartbeats, a respiration measure can be seen and counted. Averaging for 0.5 to 2 seconds (or frequency filtering) smooths out the pulse, and allows changes in the arterial pulse size to be determined.

[0227] Arterial compartment data from exercising human subjects as determined in the previous examples were analyzed using increasing smoothing on the arterial signal, which focuses on the respiratory changes. The respiratory changes can be considered another physiological compartmental contribution (that is, a first compartment with the heartbeat, having a fundamental rate of the heart rate, and a second compartment with the respiratory effect, having with a fundamental rate of the breathing cycle).

[0228] Data are shown in FIG. **10**A-B. Here, oxyhemoglobin and deoxyhemoglobin changes over time were initially calculated as in the previous examples. However, different time constants are applied in FIG. **10**A and FIG. **10**B.

[0229] In FIG. **10**A, arterial pulse data are shown during exercise (jogging from 380 to 420 seconds into the study) and through the transition to standing still (still from 420 to 480 seconds) in graph **1010**. There is little baseline change in the blood because of the previous multi-spectral processing. There are many fine spikes, such as the spikes seen at time point **1015**, which represent the heart rate in the arterial signal. These heart rate effects are difficult to see due to the scale, but note that the oxygenated and deoxygenated heme signals are both shown. The time constant for this data is change over a 150 milliseconds with 30 millisecond data sampling.

[0230] In FIG. **10**B, the same data from FIG. **10**A are shown, but subjected to a different time filtering. Here, the data are high-pass filtered with a time constant of 2 seconds, shown in FIG. **10**B as graph **1050**. Now, the respiratory effect dominates the oxyhemoglobin curve **1052** (solid-line), but is minimally present in the deoxygenated hemoglobin curve **1057** (dashed-line). Counting these cycles shows a respiratory rate of 18 breaths in 100 seconds, or about 14/minute. Further analysis (not shown) into compartments shows the respiratory effect is seen to be isolated to the arterial compartment.

[0231] Several points are worth noting in discussion.

[0232] First, these signals can be increased when breathing hard, and therefore the size of the signal increases during hard

exercise. The signal is also increased during certain respiratory diseases, such as congestive heart failure (due to pulmonary edema), asthma (due to obstructive pulmonary disease), and choking (due to increased respiratory effort and pressure gradients). One should be able to detect and count coughing, sighs, sneezes, hiccups, and other respiratory anomalies.

[0233] Second, by adding another time-constant compartment to the data analysis, the typically 8-30 Hz respiratory signal can be isolated. Similarly, this can be done through Fourier Transform time filtering as well, as is known in the art of time-analysis.

[0234] Third, intervals can be used to derive rate, as shall be explored in more detail in a later example. For example, an estimated heart rate (in beats per minute) may be determined as 60/interval, where the interval is expressed in seconds.

Example 9

Method

[0235] The steps of an exemplary method are shown in FIG. **11**.

[0236] As noted previously, there are many ways of achieving the steps of this method, but provided a multi-spectral and/or multi-compartmental approach is used to separate the signals in order to produce a stable method insensitive to motion and/or changes in body position, whether in contact or in non-contact modes, these fall within the spirit of the present invention.

[0237] A first step is collection of the data, shown as method step **1111**. In this invention the data is either non-contact optical data or loose-fit data, with a key feature being that multiple wavelengths are used. For complex determinations, this could be 6 or more wavelengths, but for the purposes of this invention 3 or more is more typical.

[0238] Next, the data is filtered. One or more filters may be used.

[0239] One such filter is to separate multispectral data into types of tissue, shown as method step **1121**. This may be performed using a matrix fit to the coefficients for the various components using published spectral weights, as was shown earlier. Alternatively, partial least squares (PLS), principal component analysis (PCA), or iterative methods could be used in such solutions.

[0240] Another such filter is to partitioning the concentrations or features found by multispectral fitting into different compartments, such as partitioning oxyhemoglobin, deoxyhemoglobin, water, or other substances into arterial and venous compartments, shown as method step **1131**. In one example, shown earlier, using values of 70% saturation of the venous blood, and 98% saturation of the arterial blood, the oxy- and deoxy-hemoglobin changes can be seen to occur in arterial and venous compartments. This step is described more fully in Example 20.

[0241] But there are other phases that can be exploited. For example, there are also venous changes that occur during heartbeats and respirations, with slightly different time constants and phase offsets than the arterial pulse. Also, just as breathing in lowers the intra-thoracic chest pressure, which increases the filling of the heart and produces larger arterial pulses, there can be venous changes as a result of the rising and falling back pressure occurring at the frequency of respiration. Next, body motion, such as raising or lowering an arm, changing body position, or jumping, produces a change in venous blood volume in the tissue (and a smaller arterial change, as arterial blood is higher pressure in muscular arteries, while venous blood is low pressure in floppy vessels). You can see this change by eye when you lower your hand, and your veins become fuller in the back of your hand, while when you raise your hand the vessels collapse and such slow changes are also seen in the studies presented earlier. Because these occur over time, and not instantaneously, there are phases and time constants that can allow identification of additional compartments. Similarly, while the changes that occur with changes in position, or with movement, or with jumping, are largely venous changes, there are some lesser arterial changes, and more sophisticated compartment models may identify these, provided sufficient wavelengths are used.

[0242] In each of these cases (heartbeat, respiration, body position changes, movement, and impact from exercise), treating the tissue as having one or more arterial changing component and one or more venous changing components allows for a method of extracting and solving for each of these changes. Each of these compartments is another "unknown" to solve for, and solved by adding more wavelengths. Another unknown, baseline reflection signal, can be solved for using more wavelengths.

[0243] Another such filter is to filter in frequency space, such as to separate heartbeat from respirations (effectively two compartments), or even to separate motion (such as probe motion) effects based on their own rhythmic frequencies, as shown in method step **1141**. This was shown earlier for separation of heartbeat and respirations using different time constants, but there are many methods such as Fourier Transform or its equivalents to produce a frequency-space data set. Suppression or removal of certain frequency ranges, and back conversion to spectral data would effectively separate the heartbeat and respiratory compartments, and may also be used to remove rhythmic exercise effects, such as walking or running induced probe and body motion.

[0244] Finally, data is output in method step **1151**. Here, parameters are selected from one or more of heart rate, heart rate interval, heart rate variability, respiratory rate, respiratory depth, respiratory effort, calories expended, calories taken in or ingested, calorie balance, hydration status, time since last ingestion of fluid, step rate, sleep stage, exercise cardiovascular zone, number of heartbeats detected, occupancy count, presence of live or dead tissue, and other physiology measures.

[0245] Last, the entire process may be repeated, as shown in method step **1165**, or one or more of each of the method steps can be repeated or used to feed back into prior analyses in order to iteratively improve the results, as shown in method step **1163**. At some point, the method is ended, at method step **1167**. The ending could be a firm end to calculation, or it could be restarted as needed.

[0246] Some additional comments on the method.

[0247] First, other ways of processing can be envisioned, for example an iterative or more sophisticated model will consider the influence of each compartment on the measurement of the other (such as if the arterial component is NOT 100% oxyhemoglobin).

[0248] Second, there are other substances that can be measured. Water, for example, can be measured using water peaks (such as at 960 nm or 820 nm) or any other point provided there is measureable contribution in the absorbance signal from water. Similarly, Ethanol, cholesterol, blood lipids, carotene, even medications can be measured in this manner.

[0249] Next, heart rate can be collected as an image, allowing the heart rate to be extracted from multiple persons in an image. Thus, a single point sensor can also be used (0-D), or a linear array can be used (1-D), instead of or in addition to the image sensor (2-D).

[0250] Next, it is not required that the sensor have contact with the subject. The heart rate sensor could be a white LED mounted in an exercise machine, with an image sensor in the display panel of the exercise machine measuring the exercising subject without contact.

[0251] Next, the sensor is not limited to measuring the heart rate of a wearer or user. The image could use the same algorithms to extract heart rate from a room full of observers, such as during a poker game or a business meeting, or at an airport checkpoint.

[0252] Also, as cardio-workout is defined in terms of minutes of elevate heart rate (either above baseline, or as a percentage of maximum ideal heart rate), one could auto-calculate the minutes of cardio workout in any day, automatically, so that the user does not have to see heart rate graphs or tables, merely seeing just the minutes of ideal cardio-workout per day for example.

[0253] Also, from the above example, it is clear that multiple analyses can be performed on different regions of the sensor, allowing multiple people to have measurements such as heart rate measured for each person either simultaneously, or by selection. The approach is not limited to one target subject, nor just to the wearer of the device. The determination could be from a glasses-mounted device that displays the heart rate of those around the wearer, and displays these results for the wearer to view.

[0254] Next, image sensors could allow such data to be collected from groups of subjects in more than one location, using only the pixels for each subject studied to calculate that subjects physiology data, such as from large rooms, street corners, security lines, or checkout aisles in stores.

[0255] Next, such measurements are not limited just to heart rate. Screening for medical diseases (such as anemia, tachycardia, heart rhythm irregularities, jaundice, malaria, heart failure, diabetes, jaundice), chemical levels (alcohol, high cholesterol), or even fitness can be screened.

[0256] Next, because the measures can be broadband, the background light, which varies according to optical contact or coupling of the light to the subject, can easily be subtracted. For example, a baseline may vary widely as a subject runs and moves with a loose fitting heart rate sensor. However, once the baseline movement is corrected (all wavelengths will change, unlike the heart rate signal which involves only some of the wavelength spectral channels), the background corrected signal will more clearly show the hemoglobin-varying signal of the heart rate. This allows a non-contact measurement that is resistant to movement, motion, changes in position, changes in background light (such as running in and out of the shadows of trees), all because the broadband signal is oversampled, with excess data that allows for background light correction.

[0257] Last, because this approach involves broadband light, even background lighting can be used to extract the measures, such as room light in a meeting, or sunlight on athletes working outdoors. This can allow elimination of the white LED.

Example 10

Separation into Compartments

[0258] Now, data is further analyzed by blood compartment.

[0259] A compartment is a location distinguished by temporal or physiological features that differentiate it from other locations. For example, the skin surface (which reflects and scatters light) can be one compartment. Muscle and tissue is another. The arterial bloodstream is a third example, and it differs in many respects (pressure, oxygenation, compliance) from the venous bloodstream, a fourth example of a compartment. Any region that can be differentiated based on such temporal or physiological characteristics can be a compartment for separation, localization, and computational analysis.

[0260] As described earlier, the venous compartment which is affected more by gravity, body position, and impact, while the arterial compartment which is affected more by heart rate and respirations. Separation of these compartments with further analysis is shown as plot **1240** of FIG. **12**B. Here, arterial-only plot **1244** is shown.

[0261] One key to the compartment separation is that arterial and venous blood have different oxygenation. In this example, we assume that the arterial compartment has a heme saturation of nearly 100%, while the second, venous compartment has an oxygen saturation of 70%. This separation yields an arterial-only volume curve shown as graph **1240** in FIG. **12**B. In this graph, the artifacts and noise from body movement and probe movement are nearly gone from the arterial pulse signal. Thus, solving for different compartments therefore allows a pulsatile arterial component, with a heartbeat associated more or less with each of the arterial local maximum values, to be separated from a widely varying venous component. Note that a large change in blood volume and absorbance is only weakly seen visible in FIG. **12**A and FIG. **12**B, and further that the pulse peaks are clearly seen even at **180** seconds and after, well into movement and/or exercise, in FIG. **12**B.

[0262] This approach can be applied to human data collected under study conditions. Multi-spectral analysis of that spectral data, in this case through a matrix solution of simultaneous linear equations, yields the data shown in FIG. **12**A-B. Here, plot **1220** of FIG. **12**A shows hemoglobin concentration changes over time at the transition from stillness to exercise at **180** seconds, analyzed and re-plotted for 160 to 190 seconds with tissue contact changes and non-heme components minimized by differential analysis, plotted for changes in hemoglobin concentration over time. The oxyhemoglobin concentration (shown as solid line **1224**) and the deoxyhemoglobin concentration (shown as dashed line **1226**) can be seen to vary differently. These two plots differ in degree of change, timing of peak changes, and even frequency, which clearly demonstrates separation of different signals that change at different times.

[0263] In the calculations of this example, a simplistic but fast way to solve for the compartments was to consider venous blood to be 70% saturated, and for arterial blood to be exactly 100% saturated. Solving only for deoxygenated blood yields changes that must be only venous, as arterial blood has no venous blood in this simplistic analysis. Since venous blood is 30% oxygenated and 70% deoxygenated, the amount of total amount of venous blood changes can be calculated from the deoxyhemoglobin change plus an additional volume change of $^{30}/_{70}$th of the deoxyhemoglobin change (that is an

additional 30% volume that is oxygenated for every volume of venous blood that is deoxygenated). Removing the oxygenated component of the venous blood leaves a change in this example that must only be the arterial compartment change, which is far more pulse-driven than gravity- and body-position-driven. This allows a pulse to easily be seen, as shown in FIG. **12**B.

[0264] Several important things are taught by the above example.

[0265] First, it is important to note that such a 70%/100% assumption is not required, and even iterative methods can determine the ratios that best fit the data.

[0266] Second, mathematical methods of solving such multiple equations are known. For example, one can apply multiple linear equations, where the values in the equation are: (1) an array of measured data within each waveband, (2) the corresponding absorbances, such as blood with and without oxygen, bilirubin, water, or fat, and (3) the result vector, which yields the concentrations (or changes in concentration) over time. In such an example, if the measured data is an N-element 1-D array named B, representing the data measured at N wavebands, and the known coefficients of effective reflection absorbance (absorbance and scattering) of each of M substances at each of the N wavebands are in a M by N 2-D array (a matrix of coefficients) named A, while the concentrations of each substance to be determined are in an M-element 1-D array of unknowns called X, then the values of X can be determined as (after regularization such that the math works, such as making N=M) then X equals the matrix operation: $A^{-1}B$. The values for the array of coefficients can be found in publications, or may be experimentally estimated. Alternatively, simple algebra can be used to reduce the complexity of the calculations to mere ratios in certain conditions, or weighted nodal partial-least-squares analysis can be used for even a more complex analysis. All of these fall under the present invention if used to correct for distance and motion in a loose-fit or non-contact physiological monitoring.

[0267] As another example, the concentration changes over time can be further partitioned into compartments by time (separation based on frequency, which is different for heart and respiratory variations, for example), or by saturation (the total changes in blood volume and saturation can be analyzed as changes in multiple compartments (such as partition into a venous component of 70% saturation versus an arterial compartment of 98% saturation).

[0268] Several comments are now included.

[0269] First, it should be understood that the compartment analysis (arterial vs. venous, or gravity vs. pulse) and the substance analysis (hemoglobin, fat, water, skin) can be performed simultaneously, and that they are performed sequentially here for the purposes of clarity of illustration. Further, the analysis can be processed in an iterative manner, which optimizes the separation based on different values of arterial and venous saturation, or upon different time constants for respiratory versus cardiac function.

[0270] Next, there are other methods that can be applied to this analysis. Time filtering, such as using a Fourier Transform to place the data into frequency-space from time-space, as is known in the art of data analysis, and can separate a regular heart rate from the pulse effects of respiration, as is shown in a later example.

[0271] All of these fall within the scope of the present invention if used in a multispectral or compartmental (or both) analysis to extract non-contact or loose-fit physiological parameters such as heart rate, respiratory rate, R-R heart beat interval, pulse oximetry, or tissue oximetry, cardiac function, bilirubin levels, sweat levels, hydration status, fat/water levels or ratios, cholesterol levels, or the like.

Example 11

Rapid and Robust Determination of Rate from Intervals

[0272] Measurement of intervals, such as the interval time between peak arterial pulse timing, or the interval time between breaths, is an advantageous method to monitor rates in living subjects.

[0273] Interval measurement by optical methods correlates well with measurement of intervals via the gold-standard EKG, as shown in FIG. **13**. Here, data from another human subject undergoing an exercise protocol and measured by both optical and electrical methods are shown. Plot line **1353** is the best-fit linear plot between the loose-fit arterial compartment beat-to-beat interval, and the electrode-based EKG beat-to-beat heart interval, both plotted in seconds. The plot is very nearly linear, with a correlation (r^2) between both measures of 0.94, showing the measure is accurate during exercise. From each of these points, an estimated heart rate (in beats per minute) may be determined as 60/interval, where the interval is expressed in seconds.

[0274] Use of intervals in order to determine rate allows for several advantages.

[0275] First, consider a heart rate of 115 beats per minute. This would be an interval of 0.52 seconds between each beat, and the heart rate could be estimated by $60/T_{interval}$, where 60 is the number of seconds in a minute, $T_{interval}$ is the beat-to-beat interval, and the result is in beats per minute.

[0276] Data accumulates, as shown in FIG. **14**A-B. In the case of FIG. **14**A, the data are relatively noise free, while in the case of FIG. **14**B the data are noisy with data dropouts. Both show model data for a heart rate of 115 beats/min.

[0277] In FIG. **14**A, data are shown in table **1411**. Here, after 1.00 seconds, only 2 heartbeats have been detected; by 10 seconds, 20 beats have been detected. To count to a stable number that estimates heart rate within a few beats per minute, perhaps 20 or 30 seconds would pass, at which time 40 to 60 beats would have been counted since the start. Here, a rate of 123/min is seen in the "HR by Count" column at data point **1423**, while a rate of 117/min would be displayed (from multiplying the count of 39 times **60**, and dividing by the counting period of 20 seconds) at data point **1425**. In contrast, if an interval method is used, a heart rate of 115/min is seen in the "HR by Interval" column after only 1 second has elapsed, at data point **1435**, a time when heart rate by counting is blank. The count-based heart rate remains blank as the number of heartbeats (2 beats over 1 second) is insufficient to determine whether the heart rate is 90 (1.5 per second) or 150 (2.5 per second). This difficulty is made even worse if the signal is noisy, as it often is in real world measurements on mobile, active living subjects, as is discussed below.

[0278] The ability to determine a rate in 1 second using an interval method represents a significant improvement over counting.

[0279] First, the user can receive a heart rate estimate in as little 1-2 seconds or less. In contrast, a runner would have to wait 20 seconds to see the heart rate using a counting system. Anyone who has watched a runner pause for heart rate mea-

surement, and grow impatient standing still, knows that this is significant user experience for athletes and other users.

[0280] Second, if the process of measurement requires power, such as driving an amplifier or illuminating an LED, a good heart rate could be determined by interval by having the watch on only a few seconds each minute, as opposed to counting for much longer periods. The impact of this can be estimated. For a wristband with a small watch battery (such as the 25 mAh CR1216-type battery used in the Timex Indiglo, Timex, Connecticut), the difference between a 3 mA draw (for a typical LED) occurring only 2 seconds each minute, versus having to stay on nearly constantly for good counting, is the difference between a 250 hour (10½ day) battery life, and an 8 hour battery life.

[0281] Third, interval measures are surprisingly robust. Consider a runner with body movement that causes every 4^{th} heartbeat to be missed. This is shown in FIG. **14**B. Here, At a rate of 115 beats/minute, the interval measured is first 0.52 sec, then 0.52 sec, but then 1.04 sec including the missed 4^{th} beat in table **1451** at data point **1459**, then 0.5 sec again, 0.5 sec, and then 1.0 sec, and repeating this pattern.

[0282] By counting, only 3 beats would be seen every 4 seconds, or 90 per minute, as shown by a count of 30 beats in 20 seconds at data point **1463** which is significantly in error, and worse, medically misleading.

[0283] In contrast, using the interval method, the modal (most frequent) interval would still be 0.5 sec, for an estimated and still-accurate heart rate estimate of 115 beats per minute at data point **1479**. In fact, the 1.0 sec interval could easily be detected as being exactly twice the most frequent rate, and thus clearly determined to be a missed beat double interval. In contrast, the counting method would estimate the heart rate at approximately 90 beats/min regardless of the counting interval. An interval method is thus robust, especially one that uses modal or other filtering.

[0284] Of note, there are many ways to estimate intervals. For example, methods to detect cyclic rates such as Fourier transforms, wavelength analysis, and the like are well within the skills on one expert in signal processing.

[0285] The interval method can be applied to respiratory rates as well. In FIG. **15**, respiratory rates determined using an interval method are shown in graph **1514**. In human studies, when the respiratory rate was controlled to be 15 breaths per minute, a rate of 15/min was determined by modal interval plotting, shown as time point **1522**. When the respiratory rate was controlled to be 10 breaths per minute, a rate of 10/min was determined by modal interval plotting, shown as time point **1535**. And last, when the respiratory rate was controlled to be 7.5 breaths per minute, a rate of 7 to 8/min was determined by modal interval plotting, shown as time point **1549**.

Example 12

Measurement of Calories Used

[0286] One of the features that can be measured using this approach is calories, either calories consumed or calories expended. In this example, it is determined in part based on a function of respiratory rate, as derived in the previous example.

[0287] Measuring calories consumed is a common laboratory experiment, and is typically performed using the relationship between the calories burned and the oxygen consumed. It is known that in the production of ATP, the energy currency of the eukaryotic cells that occurs in cells, and to a large extend near the mitochondria of the cell, that oxygen is consumed in an electron transfer called the electron transport chain, involving certain enzymes including cytochrome a/a3, cytochrome c, and others. Thus, the basis of calorie measurement in the laboratory is typically a measure of the amount of oxygen consumed, easily measured by flowing a controlled amount of oxygen into an exercise rebreathing setup that uses a closed breathing system.

[0288] It is an important realization that in this process, carbon dioxide is also produced. However, in laboratory systems, the carbon dioxide is often scrubbed away, such as by using alkaline agents that react with free carbon dioxide which the carbon dioxide reacts with. While typically ignored this carbon dioxide will become important later.

[0289] Another important realization is that the mammalian respiratory rate (at least as well studied in humans) is driven strongly by acidity of the blood and carbon dioxide levels. In contrast, oxygen does not drive respiration, save in certain end-stage lung disease. Humans placed in low oxygen airplanes at altitude will often lose consciousness before responding to their own low oxygen. Our realization includes that because reparatory rate is driven by carbon dioxide more than oxygen and carbon dioxide is produced in proportion to calories consumed, that the respiratory rate is related to calories. The final step is since we have demonstrated how to measure respiratory rate in a noninvasive, noncontact manner, that this measure can be used to estimate calorie consumption in an active, healthy person, such as during exercise using a wearable sensor.

[0290] Deriving a relationship between calories used and respiratory rate requires establishing multiple relationships. Some of these relationships have been determined, often for reasons having nothing to do with the real time monitoring of calorie consumption.

[0291] Layton (1993) developed new methodology for estimating breathing rates to determine doses resulting from exposure to airborne gases and particles. In this case, calories were not the goal of this research, but rather Layton was looking to develop scales for toxicity. Breathing rates were related to oxygen consumption associated with energy expenditures utilizing a ventilatory relationship that related minute volume to oxygen uptake as given by the equation $V=E\times H\times VQ$ (where V is ventilation in L/day, E is energy expenditure in kcal/day, H is volume of oxygen consumed in the production of 1 kJ of energy in liters of oxygen/kcal, and VQ is the "ventilatory equivalent"). H is taken to be 0.21 liters of oxygen per kcal based on a 1977-1978 Nationwide Food Consumption Survey (USDA, 1984) and the NHANES II study (US DHHS 1983). VQ is taken to be 27 (unitless) representing the ratio of minute volume to oxygen uptake, a value is derived by Layton from published data of five researchers (Bachofen et al. 1973; Grimby et al. 1966; Lambersten et al. 1959; Saltin and Astrand 1967; Salzano et al. 1984). Layton's equation was later supported by the OEHHA Report (2000).

[0292] We want to estimate calories based on respiratory rate. To begin, we modified Layton's equation for our purposes to solve instead for energy expenditure in kcal/min, instead of solving for minute ventilation, as: $E=V/(H\times VO)$. By doing this we asking a different question from the investigators interested in calculating respiratory exposure. However, the relationship between minute ventilation and respiratory rate was not clear.

[0293] To estimate minute ventilation given a respiratory rate measured by the device, we modified the work of Naranjo

et al. (2005) who demonstrated a curvilinear relation between respiratory rate and minute volume expressed by an exponential function. This study recruited trained athletes and tested them on two different treadmill protocols. Expired air was collected and analyzed for carbon dioxide and oxygen, as well as liter flow. From this they determined one relationship between tidal volume, inspiratory and expiratory duration, and respiratory rate. A nomogram was developed for a relation between tidal volume (y) and respiratory rate (x) in this group of trained athletes, with a split by phenotypic gender: $y=9.6446\ e^{0.9328x}$ for women, and $y=8.3465\ e^{0.7458x}$ for men.

[0294] The work of Naranjo addresses only breathing patterns in one group of subjects, but makes no association with calories consumed and the approach fails for subjects breathing at low rates and in non-exercise conditions.

[0295] We modified Naranjo's relationships to derive new functions to estimate energy expenditure (in kcal/min) from respiratory rate (in breaths/min) for both men and women. In one example, this relationship was best represented by second-order polynomial equations where the minimum values are the predicted resting metabolic rate, as follows: $y=0.0044x^2+0.0798x-0.2106$ for women ($r^2=0.998$) and $y=0.0069x^2+0.0463x-0.0324$ for men ($r^2=0.999$). The ability to accurately, non-invasively quantify respiratory rate allows us to combine disparate research to develop a novel solution to measuring metabolism in real-time.

[0296] Using these equations, we can now display real-time estimates of calories consumed, using the respiratory rates determined using the method of the previous example, and the calorie conversions as determined in this example.

[0297] Results from a human subject are shown in FIG. **16**. Here, cumulative calories were calculated, and could be displayed in real time on a wearable watch. A plot of one subject's data is shown as graph **1617**. At time point **1623**, the subject is breathing more quickly, and this is reflected in a more rapid increase in calories expended, as shown at time point **1625**. As the breathing is slowed, there is slower accumulation at time point **1633**. Last, at the slowest respiratory rate, the accumulation is slower still at time point **1645**.

[0298] Several points of note.

[0299] First, in contrast, some known devices for estimating calories use accelerometers (e.g., Fitbit Flex, Fitbit, San Francisco, Calif.). These devices estimate a calorie consumption using baseline calculations (such as Basal Metabolic Rate, or BMR) from age, weight, height, or other biometrics, and augment those using additional calories based on movement. These devices do not incorporate noninvasive and/or noncontact measures of respiration. And when moving only part of the body, such as when riding a stationary cycle, such devices underestimate calorie use. However, the accelerometers used in such devices could be incorporated into the present device to provide additional, supplemental data to the optical respiration measures within the spirit of the present invention provided that noninvasive and/or noncontact respiratory signals are incorporated into the analysis.

[0300] Second, in additional contrast, some other known devices for estimating calories use global positioning (GPS) signals and map data to calculate a distance traveled over time, (e.g., Runtastic, San Francisco, Calif.) and also input such as mode of movement (walking, running, skating, cycling, etc.) in order to estimate calories used. Such GPS and map data could be incorporated into the present device to provide additional data to the optical respiration measures within the spirit of the present invention provided that noninvasive and/or noncontact respiratory signals are incorporated into the analysis.

[0301] Third, a respiratory measure is a robust measure of calories. When working at high effort, our respiratory rate naturally rises to provide the ventilation required. But such a high rate is difficult to "fake." If a high rate of breathing is attempted when at rest, the carbon dioxide levels in the bloodstream will rapidly fall away from normal values, resulting in alkaline blood, changes in brain blood flow, lightheadedness, and even loss of consciousness.

Example 13

Measurement of Calories Consumed and Calorie Balance

[0302] In addition to calories used or expended, the number of calories ingested is an important part of the equation. Here, the calculations of Example 4 are relevant. Fat has an absorbance peak at multiple points, including local peaks at 760 nm, 920 nm, and elsewhere. By detecting changes in the peaks of the fat levels, and integrating over time, a measure of the fat calories consumed can be estimated.

[0303] One exemplary method would be to then assume that fat comprises a fixed amount of dietary calories, and total calories ingested can be estimated as Intake (in kcal or kJ)$=C_{in}/F_{fat}$, where C_{in} is the estimated total calories ingested, and F_{fat} is the fraction of calories estimated to come from fat.

[0304] Once calories used and calories ingested are calculated, a calorie balance over the day can be determined as: $C_{bal}=C_{in}-C_{used}$, where C_{bal} is the calorie balance over a period of time, C_{in} is the estimated total calories ingested, and C_{used} is the estimated total calories used. In this way, a user could adjust the calories consumed by eating and drinking to balance the calories burned or used during the day.

Example 14

Measurement of Hydration

[0305] In addition to calorie balance, other balances are important to a user. For example, the water balance could be calculated. Again, using the calculations of Example 4, water concentrations can be calculated. Here, water has absorbance peaks at multiple points, including local peaks near 960 nm and elsewhere (as also shown in the water spectrum of FIG. **18**), and second differential peaks near 820 nm. By detecting changes in the peaks of the water levels over time, a measure of the hydration of the subject may be determined.

[0306] For example, dehydration will lower the water content at the skin, in the tissues, result in a higher hemoglobin concentration in the blood and capillaries, and reduce the perfusion of the capillaries. In contrast, a drink of water or fluids would, when absorbed, result in the opposite: an increase in the sweat water content at the skin, an increase in the water in the tissues and capillaries, and a drop in hemoglobin concentration in the blood and capillaries, increases in perfusion of the capillaries.

[0307] A time since last hydration can be determined, and an automated detection of intake can be determined. In such cases, the time since the last drink can be calculated and displayed. Alternatively a light can be displayed that indicates a sip of fluids is needed in response to time passage or fluid losses.

Example 15

Ambient Light

[0308] As an example, the hemoglobin pulse is shown from a signal collected in ambient light in FIGS. **2**C and **2**D. An embodiment of the present invention was made omitting white LED **103** shown in FIGS. **2**C and **2**D. In addition, an embodiment was made in which the software was able to shut off white LED. Both of these systems achieved a reduction in power, with current dropping over 2 mA, for a savings of 10 mW at a 5 v LED drive voltage from having the white LED off Data were collected from the hand of a human subject at a distance of approximately 10 cm, in order to allow the room light to reach the skin and eliminate any shadow from the sensor board over the target sample tissue site.

[0309] The signal is clearly visible as peaks (for example, peaks **1722** and **1728**) where collected from distance of 10 cm from the subject in ambient light. Such signals can be processed as described in earlier examples to separate signals into various compartments and determine pulse and respiratory rate, such as is illustrated in the flow chart of FIG. **11**. Depending on the number of wavebands selected, and their range, such signals can be used to extract heart rate, respiratory rate, heart rate variability, respiratory rate, calories, hydration, sleep state (based on rate and variability), even blood alcohol or blood fat levels.

Example 16

Sleep Stage

[0310] Many sleep-stage bands collect accelerometer data. Such devices determine sleep stage by motion, which can be very inaccurate. In contrast, heart rate, heart rate variability, and respiratory rate also fit into these equations. Once a good measure of heart rate, heart rate variability, and respiratory rate is obtained using the methods described herein, sleep stage can be extracted using the equations and methods from the published literature. More accurately, a database can be assembled using remote monitoring from the optical devices disclosed herein, and the features extracted can be used to determine sleep stage using any depth of sleep algorithm known in the art.

Example 17

Complexity of Body Absorbance

[0311] The complexity of light absorbance in the body is not straightforward, which is one reason that use of a limited number of wavelengths will fail to correct for the many substances in the body, particularly if there are rapid changes in absorbance caused by drifting LED lights (less of an issue with filter-coated detectors and broadband light sources).

[0312] For example, with regard to FIG. **18**, here we show the spectra of just a few substances in the body, including water, bilirubin, hemoglobin proteins with and without oxygen, fat, and water. Use of spectral analysis, such as simple peak size detection to multispectral fitting, can allow these various components to be separated. In general, unless a method can be found to suppress a signal (such as using time-varying pulsatility to focus on certain compartments such as the bloodstream, or saturation-separation to focus on arterial vs. capillary vs. venous compartments, or use of wavelengths where the spectral contribution of the interfering substances can be minimized), the signal remains complex.

[0313] Here, the peaks of water, fat, and hemoglobin have been described earlier. For example, water has a broad peak at or near 960 nm (peak **1825**) that differentiates water from the absorbance of fat, hemoglobin with or without oxygen, bilirubin (the pigment of jaundice), and other substances. Similarly, fat content can be determined using the 920 nm fat peak (peak **1833**). This peak is often accompanied by a peak near the 760 nm peak of deoxyhemoglobin. Hemoglobin can similarly be solved for one or more of its multiple forms. There is a double peak for oxyhemoglobin at or near 542 and 577 nm (peaks **1842** and **1844**) and a broader single peak for deoxyhemoglobin at 560 nm (peak **1852**). Such approaches work for bilirubin (with a peak near 460 nm), alcohol (with peaks above 1 micron), cholesterol with peaks around 1.7 microns), and other pigmented components in the bloodstream.

[0314] The same approaches that allow determination of solutions of equations or functions that produce concentrations for water, fat, and hemoglobin can be used to extract spectral information from other substances at other wavelengths, including proteins, DNA, alcohols, chlorophyll, and other pigmented substances. The wavelengths required for analysis can be in the ultraviolet, visible, or even infrared wavelengths, provided that spectral features exist allowing extraction of concentrations or solutions to equations that are a function of the presence, absence, change, concentration, or variance in those substances over time.

Example 18

Skin-to-Sensor Distance Change with Movement

[0315] Just as a normal heartbeat leads to a pulsatile, rhythmic increase in the amount of arterial blood in certain tissues (and thus an increase in the absorbance of light, as shown in the prior example), other events can also significantly change the amount of light reflected by a tissue such as skin. For example, merely moving the skin on which a light shown farther away or toward a sensor will change the amount of light returning from the skin tissue.

[0316] We constructed a research probe that allowed the sensor shown in FIG. **2**D and a light source to be attached to a loose wristband, with data collected at many wavebands, in accordance with the present invention. This research probe allowed measurements to be collected over a wide range of wavelengths. Data were then collected with this system on a human subject with a sensor placed within 1 cm of the skin. Then the sensor was moved away from the skin, then toward the skin again, and this cyclic movement was repeated for a total of 3 cycles.

[0317] Data from this study are shown in FIG. **19**A-B. The 3 movement cycles are visible in graph **1920** of FIG. **19**A as plot line **326**, where the absorbance of light is plotted relative to a reference standard (in this case, conventional foamed open cell Styrofoam, known to provide similar scattering to tissue with an absence of spectral features). Here, absorbance begins at a low at time point **1931**, rises to a local maximum as the sensor is pulled away from the subject's forehead at time point **1933**, the falls again as the probe as moved closer again to another local minimum at time point **1935**. This pattern in the data is seen to be repeated twice more, for a total of movement through 3 absorbance cycles.

[0318] Note that the movement of the probe away from, then back toward, the subject's skin produces an apparent

change in total absorbance in this single-waveband plot (e.g., data are plotted using just one color band such as 560 to 570 nm, or after measuring just one intensity across all colors in a camera sensor over time). This matches the number of movement cycles in the study.

[0319] Importantly, this cyclic pattern caused by the movement in FIG. **19**A is in many ways similar to the cyclic pattern caused by the heartbeat seen previously in FIG. **5**A-B. In fact, if the subject's heart rate were about 60 beats per minute, and someone was jogging with a loose-fit sensor such that the cyclic movement of the sensor occurred at a similar frequency, the pulse curves of FIG. **5**A-B might be virtually indistinguishable from the body movement intensity curve in FIG. **19**A. Worse, if the jogging rate and the heart rate were different, it might be difficult to determine which is the pulse and which one is the distance movement when using just this one single-waveband plot line (this is shown at one wavelength only, but when adding additional wavelengths in accordance with the present invention the problem is solved, as shall be shown).

[0320] Because hemoglobin can be determined using spectroscopy at multiple wavelengths, and the spectrum of the skin by itself is different than the spectrum of blood, multiple linear equations can be solved to partition the signal into blood and into skin contributions. In this example, we use the fact that hemoglobin absorbance is 100-fold higher at in the 500-600 nm range than it is in the 650-700 nm range, whereas the scattering of skin is more nearly equal over that range. By relying upon the differing absorbance of each tissue at different wavelengths, a multi-wavelength system allows separation of the signal into blood and skin tissue quantities, or even into oxygenated, deoxygenated, and non-blood tissue quantities.

[0321] The result of this multispectral approach is shown in the results shown in graph **1940** of FIG. **19**B. When skin correction is performed using additional wavelengths at which hemoglobin is not significantly absorbed, and the effect of skin proximity is calculated and removed from the data using multispectral analysis, the results look very different than those seen in FIG. **19**A. Here, plot line **1946** shows that after removing skin and distance effects, the movement artifact is reduced by nearly 100-fold, and only small variations remain (not even large enough to even show well in this plot). The remaining smaller temporal variations can be used to extract heart rate, as will be shown in later examples. Addition of even more wavelengths, selected for their ability to discriminate between blood and skin, improve the separation even more, such as with correction for body position changes, as is discussed next.

[0322] In some cases, reduction of the noise by half (an improvement in signal to noise of "one bit") may be sufficient. In this case, the reduction is by more than 90%, or roughly 7 effective bits of signal to noise improvement.

Example 19

Body Position Change

[0323] Again, just as both the heart beat pulse and probe movement each lead to a change in the amount of various components of the bloodstream (in these examples, blood and water), and thus leads to changes in the absorbance of light, positional changes of the body are yet another factor that change the amount of light returning from the body.

[0324] For example, by merely raising your arm above your head, or by lying down then standing up, one changes where the blood redistributes in the body (this is a big issue in space travel, where the blood that is normally in your legs due to gravity distributes everywhere, making your face puffy and engorged with blood). One can see this effect by dropping one's wrist at one's side, and noting the swelling up of the veins (with no similar effect easily seen on the arteries), and then raising one's hand above one's head, and noting the emptying of the veins. There is a reason for this: arteries are high-pressure, muscular vessels with little change in volume with pressure (in physics terms, arteries have a low compliance, defined as change in volume with pressure), while veins are floppy, baggy, low-pressure tubes with a large change in volume with a very small change in pressure (high-compliance). A shift in the location of various components of the bloodstream between the veins, arteries, and capillaries creates a signal that can mask the more subtle changes introduced by the beating heart and by breathing.

[0325] Data collected using the system of the previous example is shown in FIG. **20**A-B. In this study performed on a human subject, a sensor was placed within 1 cm of the skin of the wrist, but the light emitter and the light detector do not touch the skin because the light source and detector are recessed in the probe (for example, as is shown in FIG. **9**A-B). During the study, the subject is held still and stable for 30 seconds, then the wrist is moved up in the air above the head and held for 30 seconds, then brought back to waist height and held for the seconds, and this movement cycle is repeated for 1 additional cycle.

[0326] These 2 movement cycles are visible in graph **2040** of FIG. **20**A. Here, the absorbance of light is again plotted relative to a reference standard as plot line **2046**. The absorbance begins at a high at time point **2051**, representing data when the wrist has not be raised and has been in the same position for several minutes, such that the absorbance remains stable through time point **2053**. Next, the data spikes at point **2055** then falls rapidly to a local minimum at time point **2057** as blood drains from the wrist, then rises again as the wrist is once again raised at time point **2059**, continuing to rise through point **2062**, then spiking again at point **2064** and falling again at time point **2066** as the wrist is again dropped though rising slowing by point **2068**.

[0327] Several points are important to note.

[0328] First, a loss of signal (increased absorbance) with moving away from the skin makes intuitive sense. If bodies remained at rest, then such measurements could be straightforward. But when considering only one wavelength, it is difficult to determine whether a change in intensity is a change in the proximity or contact with skin, or a change in blood volume in the tissue, or a change in the blood content from a heartbeat. More violent movement, such as impacts during running and jumping, product strong changes that make heart rate detection very difficult to perform accurately at one wavelength, except in certain circumstances or with addition of additional monitoring data.

[0329] Second, the same pattern (falling with raising of the wrist, rising with lowering of the wrist) repeat each cycle, showing these general changes are a result of body movement. While a moving probe can be corrected with a tight wristband or well stabilized probe, the body will move in position during exercise, making this change difficult to correct for. Many commercial probes correct for this by being not only fixed in place with a strap to prevent probe movement

and ambient light seeping under the sensor, but also are sufficiently tight so as to reduce venous blood flow. Such approaches cannot be used in a non-contact loose-fit or remote monitoring device, and they fail under such circumstances with movement.

[0330] Third, a rising and falling pattern is the same type of signal produced by the heartbeat, which can make the signals hard to separate if the body motion and movement is rhythmic and occurs at a rate that a heartbeat would be expected to occur (such as a once a second movement from footfalls during running). The size of the absorbance change with movement is on the order of 0.05-0.15 absorbance units. This is 100 fold larger than the changes due to the heartbeat. As changes in body position are common during jogging and other exercise, and if rhythmic can be very similar to the heartbeat curve seen in FIG. **5**A-B, the large size presents additional barriers to uncovering the heartbeat.

[0331] Using multiple wavelengths, the same correction for changes in distance to the skin shown in Example 18 was performed, and the data as shown in FIG. **20**A is re-plotted after correction, as shown in graph **2080** of FIG. **20**B. Unlike in Example 18, the skin correction does not eliminate most of the large swings in absorbance. In fact, the absorbance still begins high at time point **2081** (compare time point **2051** in FIG. **20**A), still spikes at point **2085**, then falls rapidly to a local minimum at time point **2087** (compare time point **2057**), rises again at time point **2085** (compare time point **2055**), falls again at time point **2087** (compare **2057**), and rises at time point **2089** (compare time point **2059**) as the wrist is again dropped.

[0332] As before, reduction of the noise is by more than half (absorbance changes up to 0.15 in FIG. **20**A, but only up to 0.05 in FIG. **20**B, an improvement in signal to noise of 1 to 2 bits). Such an improvement may be sufficient for certain applications.

[0333] So, it may be asked why didn't this skin correction work in the same way in this example as it did in Example 18. The answer has to do with physiology of compliance. When one puts one's hand down low, the blood distributes by gravity into the arm and the absorbance increases. This represents not just a change in skin contact and distance, but an actual change in the blood content of the measured skin as well.

[0334] To solve for blood changes, one needs to solve for the presence of blood (or water), or in more detail solve for the presence of oxy- and deoxy-hemoglobin. When just the skin effect is considered, this totals either 2 or 3 unknowns without separation into compartments.

[0335] In general, the number of unknowns to be solved for means that at least the same number of equations is needed to solve it well (in mathematics, it would be said N wavelengths are needed to solve for N unknowns, in order to not be underdetermined). Our biggest unknowns so far are the amount of hemoglobin and skin reflection/scattering, which requires at least 2 wavelengths. In order to determine oxyhemoglobin, deoxyhemoglobin, and skin, at least 3 wavelengths are required to solve this data set well. This is a simplification, as arteries have both oxygenated and deoxygenated blood, and there are other substances that absorb light. But there are also wavelengths were water absorbs well, so a pulse could come from the water signal instead of the amount of hemoglobin. In the next example, it will be shown how blood movement, as opposed to the probe movement, can be more completely corrected.

[0336] It is worth noting that while the predominate change in the data in FIG. **20**A-B is a blood volume change, there does appear to be certain changes that are due to contact with the skin distance as well. Note the upward spike at point **2055** in FIG. **20**A, which occurs when the wrist is thrust high into the air. This change is not only in a different direction than the fall in absorbance that occurs with blood draining from the arm after a raising of the wrist, but it also has a different time component. However, correction of the skin changes in FIG. **20**B shows that the spike at the same time point is nearly gone after skin correction at time point **2085**. This suggests that the spike at the start is not a blood change, but rather movement of the loose fit bracelet. A similar spike appearing in FIG. **20**A at time point **2064** is also nearly gone in FIG. **20**B at time point **2094**. This suggests that a multi-wavelength correction may be required during physical exercise and movement as both skin and blood distribution changes will occur with motion.

[0337] In the next example, it will be shown how movement of blood in the body can be corrected for, and used to enhance the heartbeat signal.

Example 20

Rejecting Blood Movement Using a Compartment Model

[0338] So how does one solve correct for blood movement, given that water and hemoglobin are present in all the compartments? The answer is to consider physiology.

[0339] Movement of blood during body movement tends to occur in the veins. This is because veins tend to be floppy, thin, low-pressure tubes that are partially distended with blood, and therefore swell and empty small changes in pressure, such the column of pressure created by gravity. In contrast, there is a much smaller change in the arteries. Arteries are thick and muscular, and are already under substantial blood pressure. Therefore, when the body moves, gravity does not cause them to empty or fill very much. Because movement under gravity occurs more in the veins than in the arteries, this allows multi-wavelength analysis to include another "compartment" in the analysis: what is that some of the oxyhemoglobin and deoxyhemoglobin is in the veins, and some is in the arteries.

[0340] Now, if arterial and venous blood were identical in composition, this floppy versus stiff tube approach would not add much useful information. However, arterial blood and venous blood different in many important ways: pH, oxygen content, dissolved carbon dioxide, and other ways. Venous blood, for example is typically 70% oxygenated in healthy adults at sea level (that is about 70% oxyhemoglobin, 30% deoxyhemoglobin, not including smaller amounts of other heme forms typically totaling under 2% of the hemoglobin). At the same time, arterial blood is typically about 95-99% oxygenated in healthy adults at sea level (that is, about only 1-5% deoxyhemoglobin, and the rest is oxyhemoglobin, again not counting other heme forms present).

[0341] These physiological and compartmental differences in oxygenation allow the measured components to be sorted into multiple compartments (e.g., arterial, venous, skin, muscle, gut, and liver). For example, skin is where melanin and other pigments not typically seen in blood are concentrated, while muscle is where myoglobins are typically found.

In contrast, hematin, a form of hemoglobin found in malaria victims, is typically found in red blood cells in the bloodstream.

[0342] Now, rather than use just a few wavelengths, we can determine a heart rate from data collected 30 to 100 times a second from a spectrally resolved system with 6 to 8 wave bands, to which we will apply a method of multi-compartment multi-spectral analysis.

[0343] Data were collected using the research system of the of the previous example on a human volunteer undergoing exercise protocol that consists of a series of actions performed for 1-3 minutes each: sitting, abruptly moving arms while sitting, standing, abruptly moving arms while standing, squats, jogging or jumping in place, standing, then sitting. This subjected the sensor to movement of the probe as well as to changes in body position.

[0344] FIG. **21** shows absorbance at **6** wavebands over 600 seconds during the exercise protocol described above, as compared to a reference standard. Plots for wavebands in the region of 500, 530, 560, 600, 620, and 700 nm are shown over time as plot lines **2122**, **2124**, **2126**, **2128**, **2130**, and **2132**, respectively. These wavelengths are shown for reasonable detection of hemoglobin, but also for best separation on a graph for illustration purposes. Those skilled in the art would be aware algorithms can be optimized for reduced noise, such as by selecting combinations of wavelengths that best discriminate between tissue, oxyhemoglobin, and deoxyhemoglobin (or whichever substances are of interest).

[0345] Note the wide variation in the signal with movement of the body and probe during exercise in FIG. **21**. For example, a period of relative physical stillness from 0 to 120 seconds shows relatively stable measures. During this period, the thickness of the plot lines **2122**, **2124**, **2126**, **2128**, **2130**, and **2132** comes from the heartbeat, respirations, normal physiological changes, and some background noise (there are minor differences as well due to the plotting of the lines at different widths as well, in order to allow the plot lines to be distinguished by eye in the figure). In contrast to the early quiet period over the first 120 seconds, the period from 120 to 180 shows additional fluctuation as the arms are moved, and large changes during movement, such as the transition from stillness to exercise and the transition from one body position to another For example the movement at **180** seconds into the study at time point **2144**, and at **360** seconds into the study at time point **2146**, each produces large changes in the raw signal.

[0346] After correcting for the movement of the probe relative to the skin, as shown in previous examples, then multispectral linear equation analysis at these 6 wavelengths allows both oxygenated and deoxygenated hemoglobin levels to be determined, in addition to changes in skin distance. For such analysis, 3 or more wavelengths are required to separate the 3 unknowns: tissue, heme with oxygen, and heme without oxygen signals. With multispectral data, one way to process the data is to use multiple equations with multiple unknowns, such as linear matrix fitting, an approach known to those skilled in the art

[0347] Multi-spectral analysis, in this case through a matrix solution of simultaneous linear equations, yields the data shown in FIG. **12**A-B. Here, plot **620** of FIG. **12**A shows hemoglobin concentration changes over time at the transition from stillness to exercise at **180** seconds, analyzed and re-plotted for 160 to 190 seconds using the same data plotted in FIG. **21**, only here with tissue contact changes and non-heme components minimized and plotted for changes in hemoglobin concentration over time. The oxyhemoglobin concentration (shown as solid line **1224**) and the deoxyhemoglobin concentration (shown as dashed line **1226**) can be seen to vary differently. These two plots differ in degree of change, timing of peak changes, and even frequency, which clearly demonstrates separation of different signals that change at different times.

[0348] Now, data is further analyzed by blood compartment. As described earlier, the venous compartment which is affected more by gravity, body position, and impact, while the arterial compartment which is affected more by heart rate and respirations. Separation of these compartments with further analysis is shown as plot **1240** of FIG. **12**B.

[0349] The key to the compartment separation is that arterial and venous blood have different oxygenation. In this example, we assume that the arterial compartment has a heme saturation of nearly 100%, while the second, venous compartment has an oxygen saturation of 70%. This separation yields an arterial-only volume curve shown as graph **1240** in FIG. **12**B. In this graph, the artifacts and noise from body movement and probe movement are nearly gone from the arterial pulse signal. Thus, solving for different compartments therefore allows a pulsatile arterial component, with a heartbeat associated more or less with each of the arterial local maximum values, to be separated from a widely varying venous component. Note that the large change in blood volume and absorbance seen at **180** seconds in FIG. **21** is now gone, and only weakly seen visible in FIG. **12**A and FIG. **12**B, and further that the pulse peaks are clearly seen even at **180** seconds and after, well into movement and/or exercise, in FIG. **12**B.

[0350] In the calculations of this example, a simplistic but fast way to solve for the compartments was to consider venous blood to be 70% saturated, and for arterial blood to be exactly 100% saturated. Solving only for deoxygenated blood yields changes that must be only venous, as arterial blood has no venous blood in this simplistic analysis. Since venous blood is 30% oxygenated and 70% deoxygenated, the amount of total amount of venous blood changes can be calculated from the deoxyhemoglobin change plus an additional volume change of $^{30}/_{70}$th of the deoxyhemoglobin change (that is an additional 30% volume that is oxygenated for every volume of venous blood that is deoxygenated). Removing the oxygenated component of the venous blood leaves a change in this example that must only be the arterial compartment change, which is far more pulse-driven than gravity- and body-position-driven. This allows a pulse to easily be seen, as shown in FIG. **12**B.

[0351] Several important things are taught by the above example.

[0352] First, it is important to note that such a 70%/100% assumption is not required. Iterative methods can determine the ratios that best fit the data, or tissue oximetry and pulse oximetry can be used to measure these values more precisely, allowing accurate numbers to be used in the compartmental calculations.

[0353] Second, mathematical methods of solving such multiple equations are known. For example, one can apply multiple linear equations, where the values in the equation are: (1) an array of measured data within each waveband, (2) the corresponding absorbances, such as blood with and without oxygen, bilirubin, water, or fat, and (3) the result vector, which yields the concentrations (or changes in concentration)

over time. In such an example, if the measured data is an N-element 1-D array named B, representing the data measured at N wavebands, and the known coefficients of effective reflection absorbance (absorbance and scattering) of each of M substances at each of the N wavebands are in a M by N 2-D array (a matrix of coefficients) named A, while the concentrations of each substance to be determined are in an M-element 1-D array of unknowns called X, then the values of X can be determined as (after regularization such that the math works, such as making N=M) then X equals the matrix operation: $A^{-1}B$. The values for the array of coefficients can be found in publications, or may be experimentally estimated. Alternatively, simple algebra can be used to reduce the complexity of the calculations to mere ratios in certain conditions, or weighted nodal partial-least-squares analysis can be used for even a more complex analysis. All of these fall under the present invention if used to correct for distance and motion in a loose-fit or non-contact physiological monitoring.

[0354] As another example, the concentration changes over time can be further partitioned into compartments by time (separation based on frequency, which is different for heart and respiratory variations, for example), or by saturation (the total changes in blood volume and saturation can be analyzed as changes in multiple compartments (such as partition into a venous component of 70% saturation versus an arterial compartment of 98% saturation).

[0355] As before, reduction of the noise by half (an improvement in signal to noise of "one bit") may be sufficient. However, the combined improvement of both corrections yields an estimated reduction by more than 99%, or roughly 8 effective bits of signal to noise improvement.

[0356] Several additional comments are now included.

[0357] First, it should be understood that the compartment analysis (arterial bloodstream vs. venous bloodstream vs skin surface) and the component substance analysis (hemoglobin, fat, water, skin) can be performed simultaneously, and that they are performed sequentially here for the purposes of clarity of illustration. Further, the analysis can be processed in an iterative manner, which optimizes the separation based on different values of arterial and venous saturation, or upon different time constants for respiratory versus cardiac function.

[0358] Next, there are other methods that can be applied to this analysis. Time filtering, such as using a Fourier Transform to place the data into frequency-space from time-space, as is known in the art of data analysis, and can separate a regular heart rate from the pulse effects of respiration, as is shown in a later example.

[0359] All of these fall within the scope of the present invention if used in a multispectral or compartmental (or both) analysis to extract non-contact or loose-fit physiological parameters such as heart rate, respiratory rate, R-R heart beat interval, pulse oximetry, or tissue oximetry, cardiac function, bilirubin levels, sweat levels, hydration status, fat/water levels or ratios, cholesterol levels, or the like.

SUMMARY

[0360] In summary, the improved sensors have multiple expected and unexpected advantages that can result from using broadband white LED illuminators (or broadband ambient light sources) and spectrally-resolved detectors in mobile devices, especially when combined with integrated processing power. In certain applications, such as fitness applications, this improvement may occur without undue space and size constraints, and all without degrading or with improvement in output stability. We show that improved sensors can be achieved by (a) using broadband light, from the room or from a white LED source, and (b) using a sensor with multiple narrowband spectral filters built into a portable board, such that the improved sensor can even be embedded into watches, bracelets, pendants, phones, and even clothes. Sensitivity to hemoglobin and other tissue components in various compartments allows for quantitative detection of gestures and physiology, and improves data quality during movement, allowing non-contact operation. Such improved sensors may permit a light source and detector to be embedded into nearly any mobile device, such as into a smartphone, bracelet, pendant, shoe, clothing, or watch.

[0361] We have discovered an improved hydration sensor and monitoring method for mobile, wearable, non-contact, and remote use. Various sensor implementations have been constructed and tested, in which a solid-state broadband white LED, and one or more sensors having spectral filters designed to pass certain predetermined wavebands of light to produce (if needed in the absence of adequate ambient light or to replace ambient light) a continuous, broadband light from 660 nm to 1000 nm, and a spectrally resolved detection. The resulting data is passed to a processor and memory having programs for execution by the processor to determine a measure of hydration, such as fluid losses, fluid intake, fluid balance, or perfusion, or rate of fluid losses. In one example, variations in components of the bloodstream over time such as hemoglobin and water are determined based on the detected light, and the measure of hydration status is then determined based on the in components of the bloodstream over time. In addition, the sensor is sensitive to other physiology (e.g., heart rate, respiratory rate, jaundice, alcohol levels), as well as to type and state (e.g., finger, hand, live, dead), for analysis and initiating actions based on the resulting determinations. This device has been built and tested in several configurations in models, animals, and humans, and has immediate application to several important problems, both medical and industrial, and thus constitutes an important advance in the art.

We claim:

1. A method for estimating hydration of a living subject, comprising the steps of:

(a) noninvasively detecting light, said detected light being at least in part backscattered from or transmitted through the subject;

(b) determining a measure of water content, said measure of water content at least in part based on a function of a concentration of components of the bloodstream or tissue of the subject over time determined using spectral analysis of the detected light; and,

(c) generating an output that is a function of hydration status of the subject, said output based at least in part on the measure of water content.

2. A method for estimating hydration of a living subject, comprising the steps of:

(a) detecting broadband light after interaction with the subject, and further after spectral filtering or separating said broadband light into different narrowband wavelength ranges prior to detection;

(b) determining a measure of water content, said measure of water content at least in part based on a function of a variation in concentration of components of the blood-

stream or tissue of the subject over time determined using spectral analysis of the detected light; and,

(c) generating an output that is a function of a hydration measure, said output based at least in part on the measure of water content.

3. A method for estimating hydration of a living subject, comprising the steps of:

(a) detecting broadband light arriving after interaction with the subject and after spectral filtering or separation of the broadband light into different narrowband wavelength ranges, and generating spectral data;

(b) analyzing the spectral data to computationally partition the data into more than one physiological compartment of the subject having different temporal or physiological characteristics, and into one or more blood or tissue components of the subject, said blood or tissue components including at least a measure of water content; and,

(c) generating an output that is a function of a hydration status of the subject, said output based at least in part on the computational partitioning.

4. The method of claim **2**, wherein the detected light arriving after interaction with the subject is from broadband ambient light.

5. The method of claim **2**, wherein the detected light arriving after interaction with the subject is produced by a solid-state, broadband, white LED.

6. The method of claim **2**, wherein the step of detecting broadband light occurs without physical contact with the subject.

7. The method of claim **2**, wherein the step of detecting broadband light occurs at a distance from the subject.

8. The method of claim **2**, wherein the step of detecting broadband light occurs with intermittent physical contact with the subject.

9. The method of claim **2**, wherein the output is a hydration measure selected from the list of hydration measures including hydration sufficiency, fluid loss, fluid consumed, fluid balance, rate of fluid loss over a period of time, an indication of fluid loss in excess of fluids taken in, and an indication of fluids consumed in excess of fluid loss.

10. The method of claim **3**, wherein said more than one physiological compartment comprises the arterial bloodstream of the subject, the venous bloodstream of the subject, and the surface skin reflectance of the subject.

11. The method of claim **3**, wherein said more than one blood or tissue components of the subject comprises hemoglobin and water.

12. The method of claim **2**, wherein the step of spectral filtering or separation of the broadband light comprises filtering the detected light through narrowband interference filters deposited directly on one or more detectors.

13. The method of claim **2**, wherein the step of spectral filtering or separation of the broadband light comprises filtering or separating the broadband light for detection at more than one detector or detector region.

14. A device for estimating hydration of a living subject, comprising:

(a) at least one sensor configured to noninvasively detect light being backscattered from or transmitted through the subject, and,

(b) a processor, and memory storing one or more programs for execution by the processor, the one or more programs including instructions for determining at least a measure of water content, said measure of water content determined at least in part based on a measure of changes in components of the bloodstream or tissue of the subject over time using spectral analysis of the detected light, and for generating an output that is a function of a hydration status of the subject, said output based at least in part on the measure of water content.

15. A device for estimating hydration of a living subject, comprising:

(a) one or more sensors configured to noninvasively detect broadband light after interaction with the subject, each of said sensors comprising at least one narrowband spectral filter configured to spectrally filter or separate said broadband light into different narrowband wavelength ranges prior to detection; and,

(b) a processor, and memory storing one or more programs for execution by the processor, the one or more programs including instructions for determining at least a measure of water content, said measure determined at least in part based on a computational spectral analysis of variation in concentration of components of the bloodstream or tissue of the subject over time using the detected light, and for generating an output that is a function of a hydration status of the subject, said output based at least in part on the measure of water content.

16. A device for estimating hydration of a living subject, comprising:

(a) one or more sensors configured to noninvasively detect broadband light after interaction with the subject, each sensor further comprising a narrowband spectral filter configured to be sensitive to a predetermined waveband of light, and generating spectral data; and,

(b) a processor, and memory storing one or more programs for execution by the processor, the one or more programs including instructions for analyzing the spectral data to computationally partition the data into more than one physiological compartment of the subject having different temporal or physiological characteristics, and into one or more blood or tissue components of the subject, said blood or tissue components including at least a measure of water content; and for generating an output that is a function of a hydration status of the subject, said output based at least in part on the computational partitioning.

17. A device for estimating hydration of a living subject, comprising:

(a) a solid-state broadband LED illuminator configured to illuminate a target site on the subject with broadband light;

(b) one or more sensors configured to noninvasively detect broadband light after interaction with the subject, each sensor further comprising a narrowband spectral filter configured to be sensitive to a predetermined waveband of light, and generating spectral data; and,

(c) a processor, and memory storing one or more programs for execution by the processor, the one or more programs including instructions for analyzing the spectral data to computationally partition the data into more than one physiological compartment of the subject having different temporal or physiological characteristics, and into one or more blood or tissue components of the subject, said blood or tissue components including at least a measure of water content; and for generating an output

that is a function of a hydration status of the subject, said output based at least in part on the computational partitioning.

18. The device of claim **15**, wherein the detected light arriving after interaction with the subject is from broadband ambient light.

19. The device of claim **15**, further comprising a solid-state, broadband LED for illuminating the subject with broadband light.

20. The device of claim **15**, wherein the device is further configured as part of a system selected from the list of systems including a mobile personal health monitor, a mobile phone, a wearable device, wearable clothing, wearable glasses, a wearable bracelet, wearable earphones, wearable contact lenses, a security system, a room occupancy sensor.

21. The device of claim **15**, further comprising at least one narrowband spectral filter deposited directly on the sensor, wherein the sensitivity of the sensor to different wavelength ranges is achieved using said at least one narrowband spectral filter.

22. The device of claim **15**, wherein the device is configured to operate in a non-contact manner with the subject.

23. The device of claim **15**, wherein the device is configured to operate at a distance from the subject.

24. The device of claim **15**, wherein the device is configured to operate with intermittent physical contact with the subject.

25. The device of claim **15**, wherein the output is a hydration measure selected from the list of hydration measures including hydration sufficiency, fluid loss, fluid consumed, fluid balance, rate of fluid loss over a period of time, an indication of fluid loss in excess of fluids taken in, and an indication of fluids consumed in excess of fluid loss.

26. The device of claim **15**, further comprising at least one narrowband spectral filter deposited directly on the sensor, wherein the sensitivity of the detector to different wavelength ranges is achieved using said at least one filter.

27. The device of claim **16**, wherein said more than one physiological compartment comprises the arterial bloodstream of the subject, the venous bloodstream of the subject, and the surface skin reflectance of the subject.

28. The device of claim **16**, wherein said one or more blood or tissue components of the subject comprises hemoglobin and water.

* * * * *

专利名称(译)	用于手机，智能手表，占用传感器和可穿戴设备的水合监测传感器和方法		
公开(公告)号	US20150148623A1	公开(公告)日	2015-05-28
申请号	US14/552690	申请日	2014-11-25
[标]申请(专利权)人(译)	贝纳龙DAVID ALAN		
申请(专利权)人(译)	贝纳龙，DAVID ALAN		
当前申请(专利权)人(译)	Alifak		
[标]发明人	BENARON DAVID ALAN		
发明人	BENARON, DAVID ALAN		
IPC分类号	A61B5/00 A61B5/1455		
CPC分类号	A61B5/0059 A61B5/443 A61B5/1455 A61B5/02427 A61B5/0075 A61B5/0205 A61B5/02405 A61B5/0261 A61B5/0476 A61B5/0806 A61B5/0816 A61B5/083 A61B5/085 A61B5/091 A61B5/14546 A61B5/14551 A61B5/14552 A61B5/4812 A61B5/4866 A61B5/4875 A61B5/6802 A61B5/681 A61B5/7207 A61B5/7225 A61B5/7253 A61B2560/0247		
优先权	61/908926 2013-11-26 US 62/050828 2014-09-16 US 62/053780 2014-09-22 US 61/989140 2014-05-06 US 62/050900 2014-09-16 US 62/050954 2014-09-16 US 61/970667 2014-03-26 US		
外部链接	Espacenet USPTO		

摘要(译)

用于移动设备，可穿戴设备，安全，照明，摄影和其他设备和系统中的水合监测的改进传感器（<b> 102 </ b>）使用可选的荧光涂层宽带白光LED（<b> 103 </ b）>）产生宽带光（<b> 114 </ b>），然后将其与任何环境光一起传输到目标（<b> 125 </ b>），例如生活的耳朵，脸或手腕学科。从目标返回到探测器（<b> 141 </ b>）的一些散射光通过窄带光谱滤波器组（<b> 155 </ b>）以产生多个探测器区域，每个探测器区域对不同的敏感波长波长范围，并且对检测到的光进行光谱分析以确定水合的量度，例如流体损失，流体摄入，液体平衡或液体流失率，部分基于血流成分的非侵入性测量。在一个实例中，基于检测到的光确定血流成分随时间的变化，例如血红蛋白和水，然后基于血流的成分随时间确定水合度。在没有LED灯的情况下，环境光可以是用于分析的足够照明。相同的传感器可以提供组织目标的类型或状态的识别特征，例如心率或心率变异性，呼吸状态，或甚至确认组织是活的。包含传感器的水合监测系统以及方法也是如此披露。